

T H E S I S

AUTHOR: K.F. WILLIAMS.

DEPARTMENT: ELECTRICAL AND CONTROL ENGINEERING.

TITLE: CLOSED LOOP STEPPING MOTOR APPLICATION  
IN PROSTHETICS.

SUPERVISOR: R. THOMASON.

September, 1969

ProQuest Number: 10832135

All rights reserved

INFORMATION TO ALL USERS

The quality of this reproduction is dependent upon the quality of the copy submitted.

In the unlikely event that the author did not send a complete manuscript and there are missing pages, these will be noted. Also, if material had to be removed, a note will indicate the deletion.



ProQuest 10832135

Published by ProQuest LLC (2018). Copyright of the Dissertation is held by Cranfield University.

All rights reserved.

This work is protected against unauthorized copying under Title 17, United States Code  
Microform Edition © ProQuest LLC.

ProQuest LLC.  
789 East Eisenhower Parkway  
P.O. Box 1346  
Ann Arbor, MI 48106 – 1346

31M

SUMMARY

An attempt is made to use a stepping motor as an actuator for an artificial limb.

## CONTENTS

	<u>Page</u>
Summary.	i
Introduction	1
1. Extent and classification of deformities.	2
2. Principles of myoelectric control and the suitability of such a control for the various deformities.	6
3. Basic physiology of the neuromuscular system.	7
4. E.M.G. signal processing.	13
4.1 Methods of detecting E.M.G. signals.	13
4.2 Surface electrode systems.	13
4.3 Three - electrode array.	13
4.4 E.M.G. signal characteristics.	14
4.5 Processing problems.	18
5. The control system.	
5.1 System considerations.	20
5.2 Description of the complete control system.	24
5.3 E.M.G. signal amplifiers.	25
5.4 Variable threshold and monostable circuit.	29
5.5 Digital to analog converter.	31
5.6 Deadband and modulus circuit.	34
5.7 Voltage controlled oscillator.	37
5.8 Steering circuit.	41
5.9 Strain gauge bridge amplifier.	42
6. Actuator.	
6.1 Stepping motor operation.	44
6.2 Slo-Syn motor specification.	44
7. Mechanical Design.	
7.1 Specification.	52
7.2 Design considerations.	52

	<u>Page</u>
8. Discussion	56
Acknowledgment	59
References	60
<u>Appendices</u>	
A1. Output impedance of bootstrapped amplifier	
A2. Frequency sensitivity of V.C.O.	
A3. Strut design.	
A4. Data sheets.	
<u>Figures</u>	
1.1 Classification of deformities.	3
1.2                    "	4
1.3                    "	5
3.1 Basic neuromuscular system	9
3.2 Potential of axon core relative to surrounding fluid during activated period.	10
3.3 Action potential outside and along axon core	10
3.4 Feedback elements of the neuromuscular system	11
3.5 Control loop for a pair of opposing muscles	12
4.2 Bioelectric source electrode system	15
4.3 Biological electric source vector	16
4.4 A typical E.M.G. signal	17
4.5 Relation between E.M.G. and load	19
5.11 The completed prosthesis	21
5.12 Initial control system	22
5.2 The complete control system	23
5.31 E.M.G. signal amplifier	27
5.32 E.M.G. signal amplifier results	28
5.4 Variable threshold and monostable circuit	30
5.51 Digital to Analog converter	32
5.52 D/A converter characteristic	33
5.61 Deadband and modulus circuit	35
5.62 Deadband and modulus circuit characteristic	36
5.71 Voltage - controlled oscillator	38
5.72 V.C.O. characteristic	39
5.8 Steering circuit	41

	<u>Page</u>
5.9 Strain gauge bridge amplifier	43
6.1a Wiring details of motor	46
6.1b Switching sequence	46
6.1c Resultant stator field	46
6.31 Logic waveforms	48
6.32 Switch tail ring counter	49
6.33 Motor drive logic	50
6.34 Power switch	51
7.21 Mechanical Assembly	54
7.22 Stepping motor and drive shaft	55
8 Torque/speed characteristic of H.S. 25 motor for different field current time constants.	58

## Introduction

In recent years much work has been done in many countries on the development of powered artificial limbs for use by adults and children with congenital deficiencies i.e. present at birth, and by amputees.

The established methods of actuating these powered limbs are either by pneumatic motors, operated from compressed carbon dioxide or by electric motors. Some designs have also used hydraulic and electro-hydraulic actuators.

In the development of the complete powered limb the following problems have also to be considered:

- (a). The design of the mechanical components and the harness for attaching the appliance to the body.
- (b). Control input units by means of which signals from the wearer operate the powered limb. Control input signals maybe either mechanical (bone movement) or electrical.
- (c). The control system mechanics, involving the type of feedback which should be used. This can be either visual feedback or sensory feedback from the forces exerted by the appliance.



## 1. Extent and classification of deformities

Prior to the thalidomide disaster limb deformities occurred occasionally in the U.K., but possibly less than ten per year were reported with gross deformities of two or more limbs. The number of children born alive and surviving with limb deformities in the U.K. as a result of the drug thalidomide is between 200 and 250 (H.M.S.O) (1964). Nearly 100 of these had severe deformities of two limbs and a further 60 involving all four limbs. In Germany between two and three thousand problems of deformities resulting from thalidomide were reported.

According to ref. | four groups of deformities can be differentiated (Figs |.1 and |.2 ). These are:

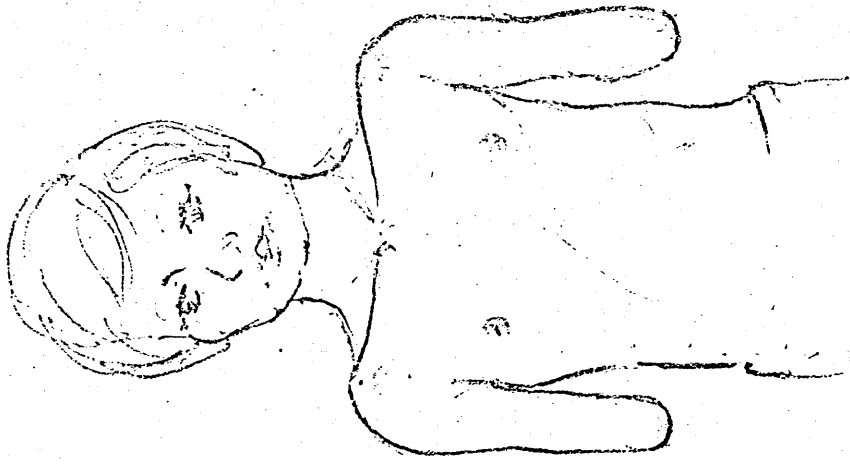
**Amelia** When the entire extremity is absent. The corresponding part of the shoulder girdle is usually under-developed but rarely absent. Small soft tissue remnants are frequently present in the area of the shoulder joints.

**Peromelia** This corresponds to amputation which means one may find a 'stump' with a square or a conical ending. Stump length and level are important for prosthetic fitting.

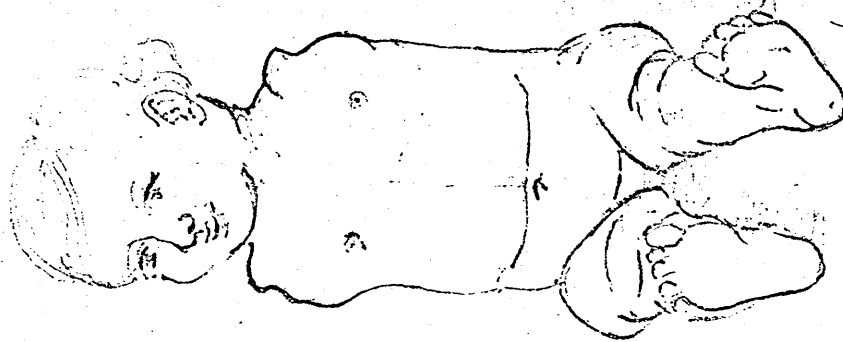
**Phocomelia** Both forearm and upper arm are absent. The hands attach immediately to the shoulder. These hands are frequently deformed and fingers maybe absent.

**Ectromelias** Represents the largest and most varied group. Variants go from absence of thumb, or a clubhand in the periphery to a pronounced shortening of the extremity, together with the proximal part being affected.

The classification for an amputee is shown in fig |.3  
(Ref. | ).

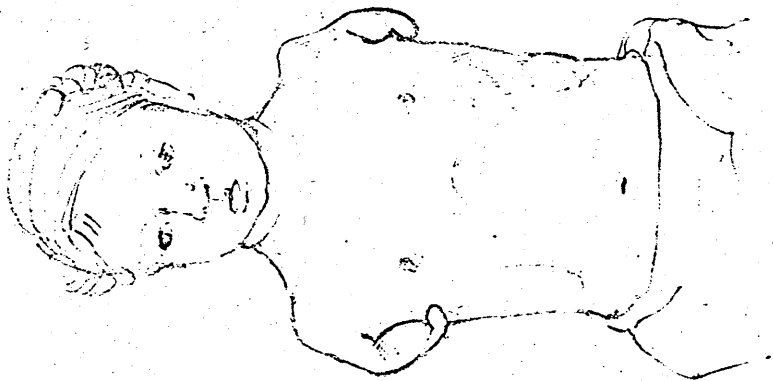


BILATERAL PEROMELIA



BILATERAL AMELIA

FIG. 1-1 CLASSIFICATION OF DEFORMITIES



BILATERAL PHOCOMELIA



BILATERAL ECTROMELIA

FIG. 1.2 CLASSIFICATION OF DEFORMITIES

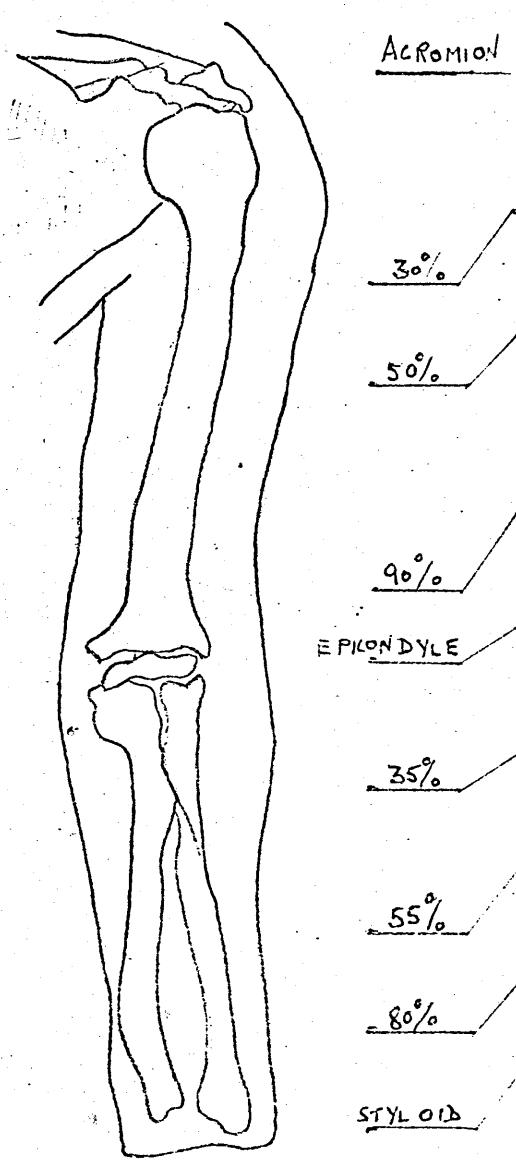
AMPUTATION LEVEL	PROSTHETIC TYPE
	SHOULDER DISARTICULATION
30%	SHORT ABOVE ELBOW
50%	STANDARD ABOVE ELBOW
90%	ELBOW DISARTICULATION
EPICONDYLE	VERY SHORT BELOW ELBOW (SPLIT SOCKET)
35%	SHORT BELOW ELBOW
55%	MEDIUM AND LONG BELOW ELBOW
80%	WRIST DISARTICULATION
STYLOID	

FIG. 1-3 CLASSIFICATION OF DEFORMITIES

2. Principles of myoelectric control and the suitability of such a control for various deformities

When a person moves a limb, electrical signals are sent along the nerves and, from there, to the muscle cells. It is these signals which 'trigger' muscle contraction. Although small, these signals may be detected at the skin using suitable amplifiers. Some 25 years ago, it was suggested that these signals might be used to control powered artificial limbs - the principle being known as myoelectric control. This type of control would be suitable for an amputee who often has healthy muscles left in his stump which are no longer connected to the missing part, or for patients paralysed by diseases such as poliomyelitis where parts of a muscle may be left, capable of giving an appreciable electrical input but too weak to move the limb.

Wholly myoelectric control of prosthesis for dysmelic children is still many years away and greater success is to be achieved with mechanical (bone movement) input position-controlled systems supplemented with some myoelectric facilities (Ref. 3 ).

### 3. Basic physiology of the neuromuscular system

A skeletal muscle is held by tendons between the bony linkages of the skeleton and is made up of thousands of muscle fibres. Each fibre being between 10 and 100 in diameter and about 5 cm. in length. These fibres are then divided up further into smaller components. Fig 3.1

A group of these muscle fibres has associated with it a single nerve fibre which originates in its nerve cell in the spinal chord. A single nerve fibre together with the bundle of muscle fibres in which it terminates is called a motor unit.

The process of stimulation of the muscle fibres is by the conduction of electrical impulses down the nerve fibres, resulting in an 'action potential'. Fig. 3.2 shows this action potential measured between the inside and outside of the nerve fibre and fig.3.3 shows the same action potential measured outside the nerve fibre. These are called respectively monophasic and diphasic nerve pulses.

Once initiated, the propagation of this action potential is invariable, progressing at a constant velocity and magnitude. The resting potential of the internal protoplasm of the nerve fibre is about 70 mV negative and the change of this potential to some 50 mV positive during the passage of an impulse represents the action potential of about 120-150 mV. The duration of the impulse is about 1 m.sec., and it propagates with a speed of some 2 to 100 metres/sec.

When a motor unit is activated by such an action potential an impulsive longitudinal force of attraction is generated in the associated muscle fibres, an impulsive longitudinal force of attraction which causes a momentary tension to develop between the ends of those muscle fibres. The quantum of muscle tension is then that tension developed by a single motor unit.

The total force of a muscle is the short-term averaging of the contractions of the many motor units presented in the muscle.

To enable the muscle to operate in a closed loop there are structures within the muscle which provide information concerning the forces at, and the positions of the skeletal linkages. These force sensors or mechanoreceptors which are sensitive to tension, lie in series with the muscle and are found in the Golgi tendon organs. These organs provide no positional information.

Information about the degree of contraction of the muscle, i.e. positional information, is provided by 'spindles' lying parallel with the extrafusal muscle fibres. These are shown in fig. 3.4

The feedback signals are taken both from the equatorial region of the spindle and towards the polar ends. These signals have a similar form to those of the nerve signals.

Both position and force feedback signals return through the nerves to the central nervous cell bodies.

A block diagram representing the control loop for a pair of opposing muscles is shown in fig. 3.5

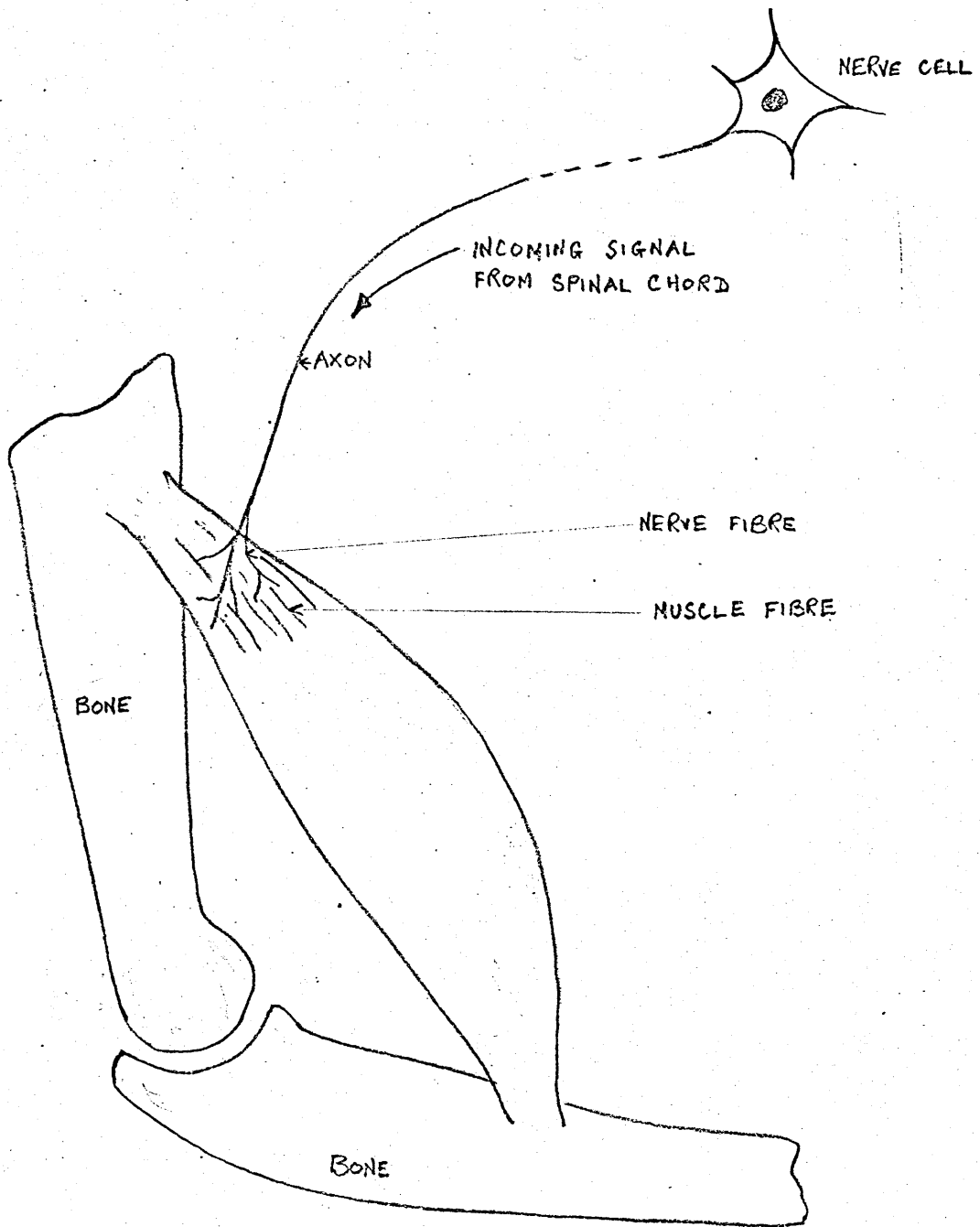


FIG. 3.1 BASIC NEUROMUSCULAR SYSTEM



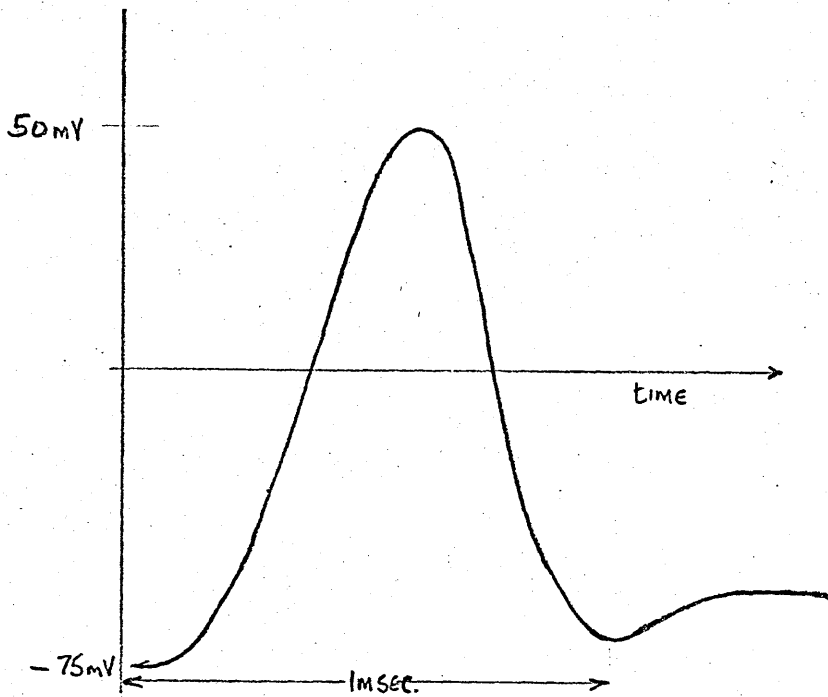


FIG. 3-2 POTENTIAL OF AXON CORE, RELATIVE TO SURROUNDING FLUID. DURING ACTIVATED PERIOD.

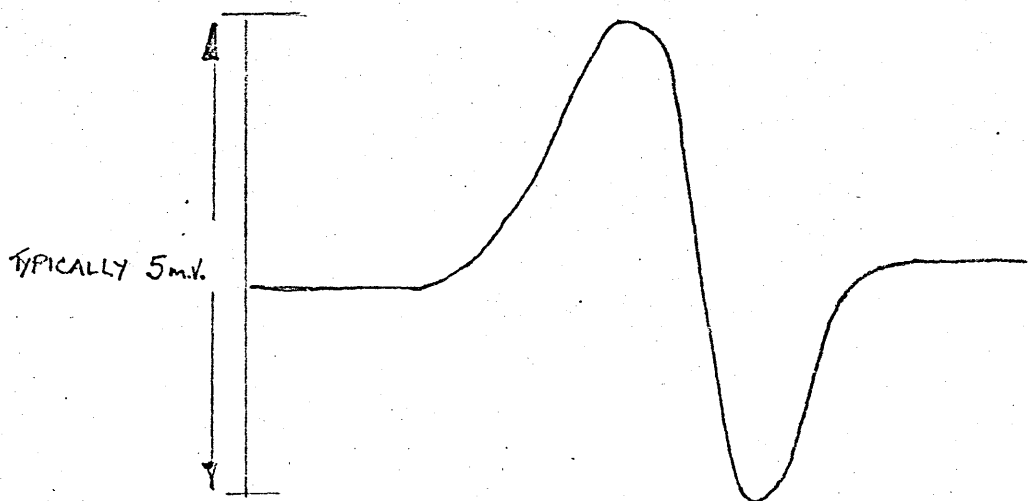


FIG. 3-3 ACTION POTENTIAL OUTSIDE AND ALONG AXON CORE.

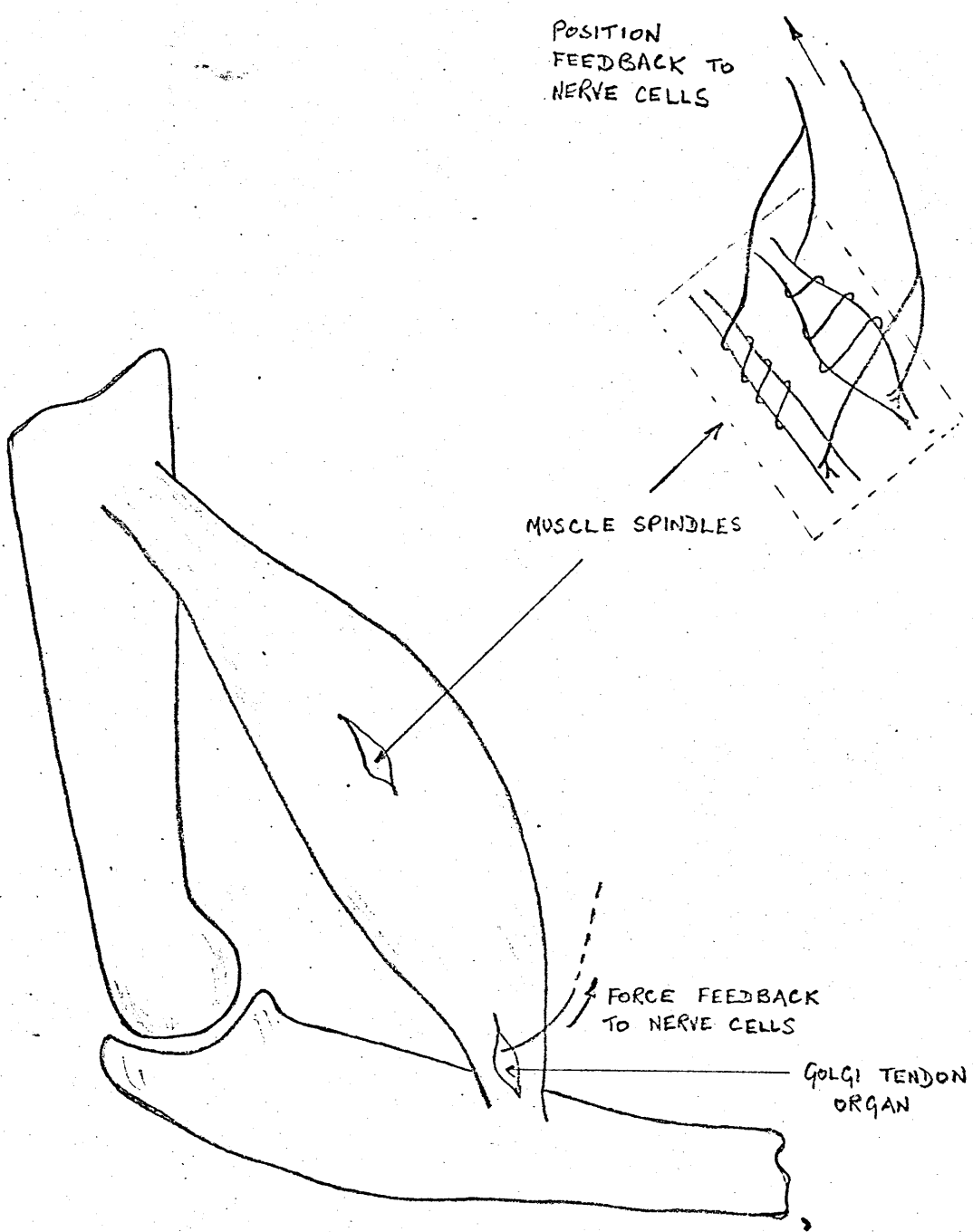


FIG. 3.4 FEEDBACK ELEMENTS OF THE NEUROMUSCULAR SYSTEM

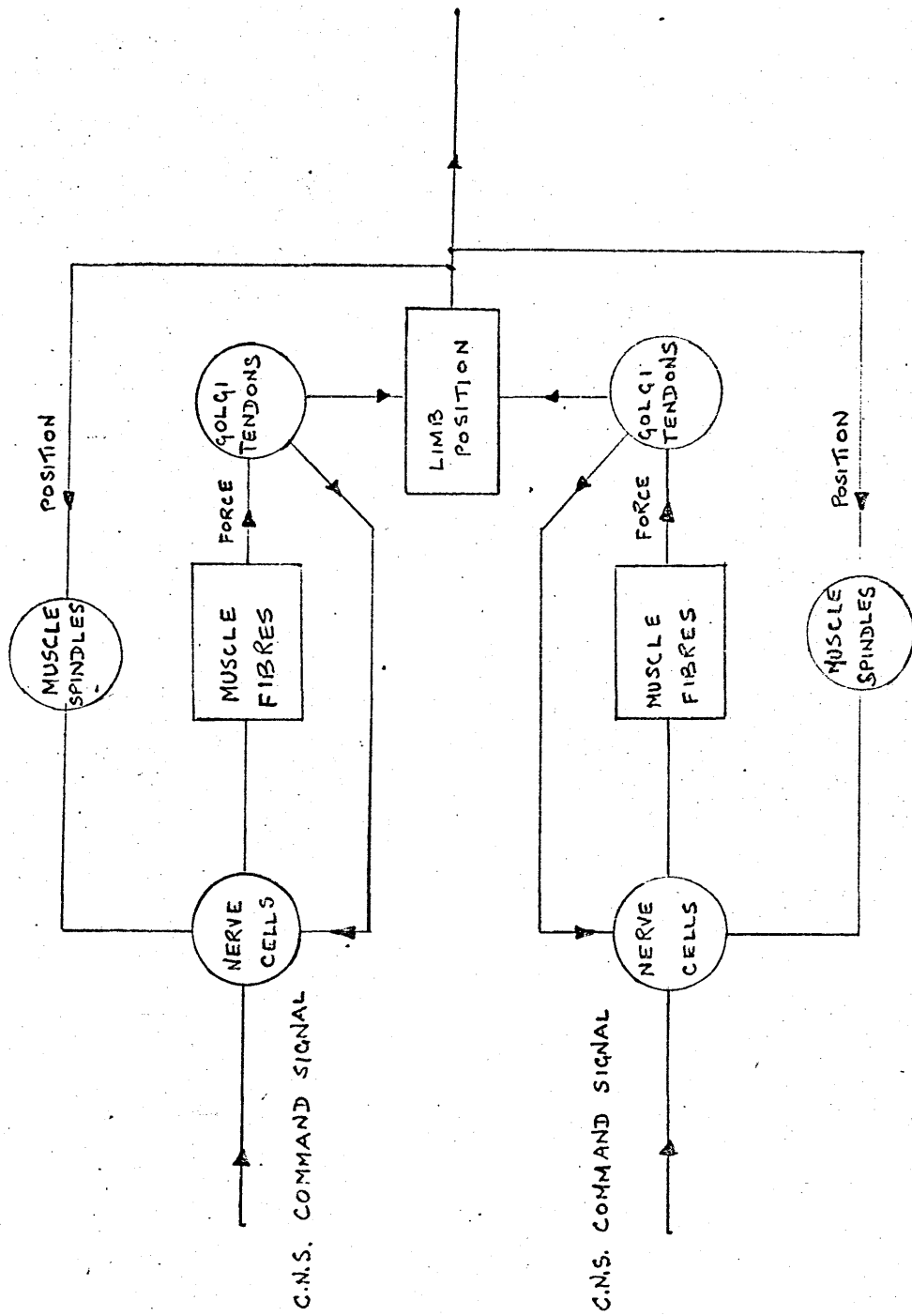


FIG. 3.5 CONTROL LOOP FOR A PAIR OF OPPOSING MUSCLES

#### 4. E.M.G. signal processing

##### 4.1 Methods of detecting E.M.G. signals

There are basically three ways of applying electrodes for E.M.G. detection. These are:

1. Under the skin - subcutaneous implants.
2. Through the skin - hypodermic electrodes.
3. Outer surface - percutaneous electrodes.

From the point of view of preparation and the skill needed for application, the surface electrodes are the simplest.

##### 4.2 Surface electrode systems

Fig. 4.2 shows a typical surface electrode in place over a layer of skin. The tissue fluids enveloped by the skin constitute an apparent electrical connection with the volume of the body and is represented in the schematic diagram by a region of low resistance. The layer of higher resistance is the layer of the skin known as the epidermis - and includes dead cells.

Contact between the skin and the metal electrode produces a metal-ionic solution interface having all the characteristics of a chemical half cell. There is a potential set up which depends on the metal, its surface, and the concentration of ions in solution. The conductive paste or saline solution used with the surface electrodes ensures a saturated concentration of halide ions and a stable half cell potential.

##### 4.3 Three-electrode array

The biological electric source is represented by a vector as shown in fig. 4.3. This vector is greatest under the skin overlying the signal source, and is attenuated as the skin surface is reached. If two pairs of electrodes are placed symmetrically over a source, the same amount of electrical activity would be expected from each pair. This is shown by the small vectors  $v$  and  $v^1$  of equal length just under the skin. Considering the outside pair of electrodes (1 and 3) the vectors  $v$  and  $v^1$  would then be added electrically.

#### 4.4 E.M.G. signal characteristics

Electrodes will in general record an aggregation of nerve, spindle and various other neuronal signals. A typical recorded signal is shown in the photograph of fig.4.4. This was recorded from the amplifier constructed. The signal has the following characteristics:

Frequency content about 10 Hz to 5 MHz

Pulse repetition frequency - increases with increased tension, varies between about 100 to 1000 pulses/sec.

Peak voltage - about 15 mV.

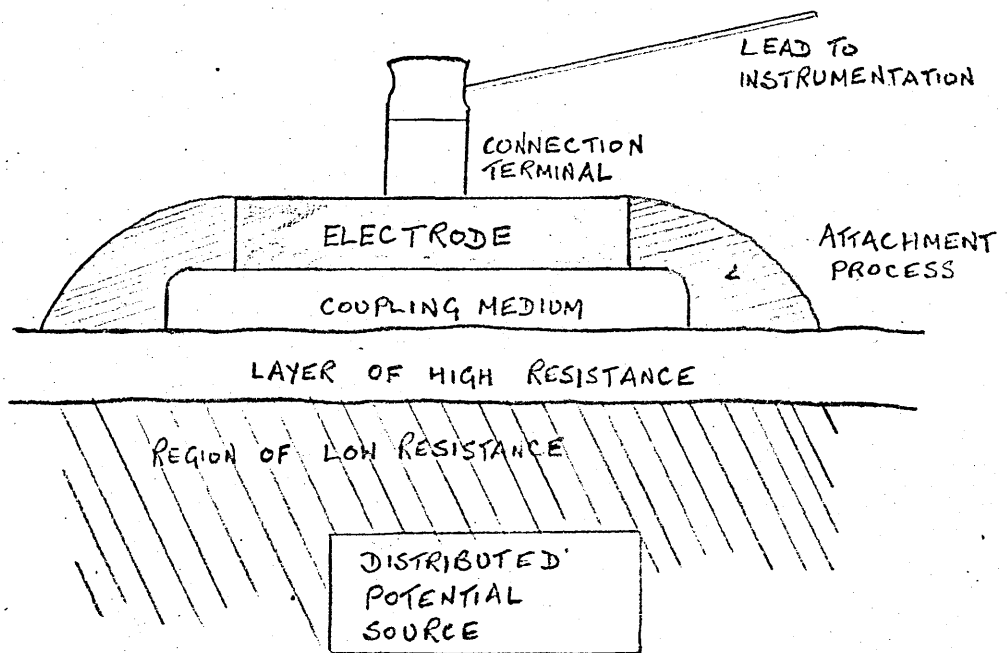


FIG. 4-2 BIOELECTRIC SOURCE ELECTRODE SYSTEM.

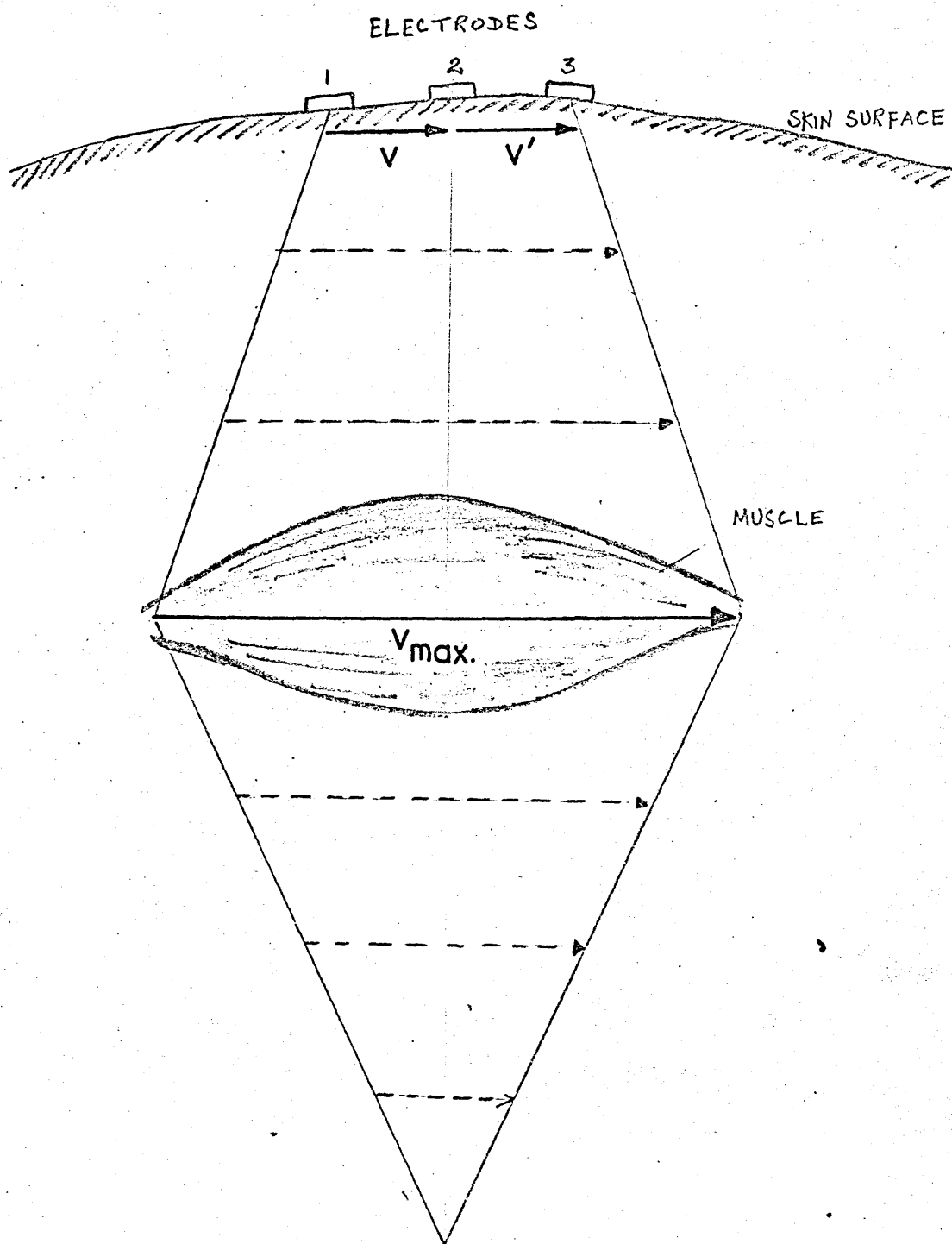
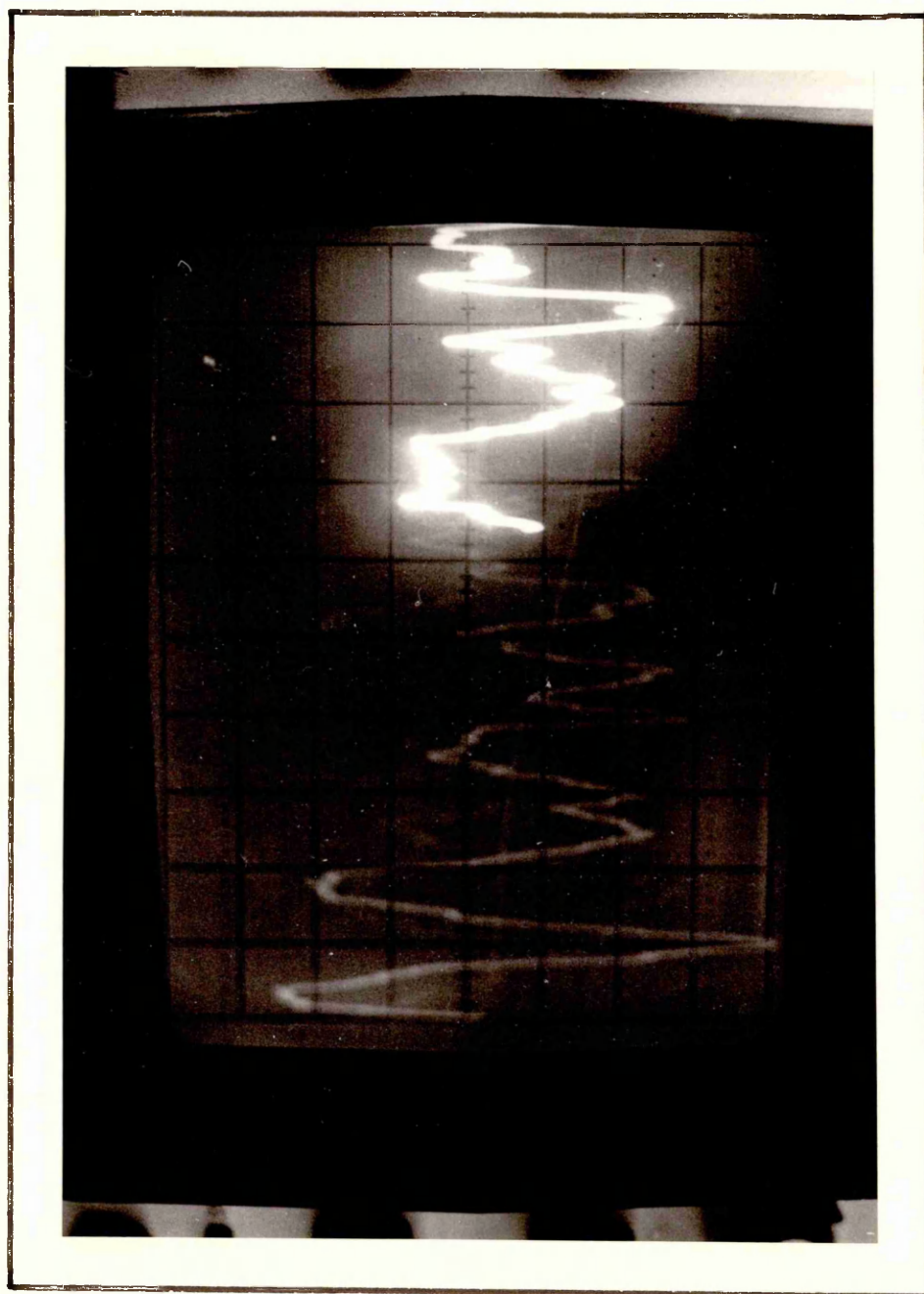


FIG. 4-3 BIOLOGICAL ELECTRIC SOURCE VECTOR



7m.v.

100m. sec.

FIG. 4-4 A TYPICAL E.M.G. SIGNAL



4.5 Processing problems

The variation of the rectified and smoothed E.M.G. signal with load is shown in fig.4.5. The relation between the E.M.G. and tension for upper arm muscles is not linear. From the point of view of using the E.M.G. as a control signal, the non-linearity is not a great disadvantage provided that there is a clear increase of E.M.G. with tension at all parts of the curve.

The E.M.G. waveform shows large irregular fluctuations in amplitude even after rectifying and smoothing. These fluctuations could of course be further smoothed out by using a longer time constant but this would result in a sluggish response when the E.M.G. is used in a control system.

The amplitude of this random variation is a function of the signal level itself usually about 20% of the d.c. level.

Another problem is that concerning the impedance of the skin. A typical value of the skin impedance between a pair of surface electrodes is a 200 K $\Omega$ . However, changes in skin resistance can be caused by perspiration and the value of 200 K $\Omega$  can drop to 5 K $\Omega$ . This can change the sensitivity of the system. A high input impedance amplifier should therefore be used.

With a three electrode system this unbalance which can be produced in the skin resistance will cause a severe drop in the common mode rejection ratio of the signal amplifier. The body acts as an aerial to any stray radiation and the received signals can be many times larger than the E.M.G. signal to be measured. It is therefore important to maintain a high level of common mode rejection.

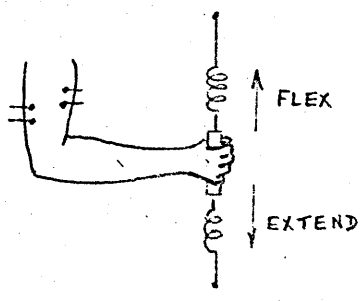
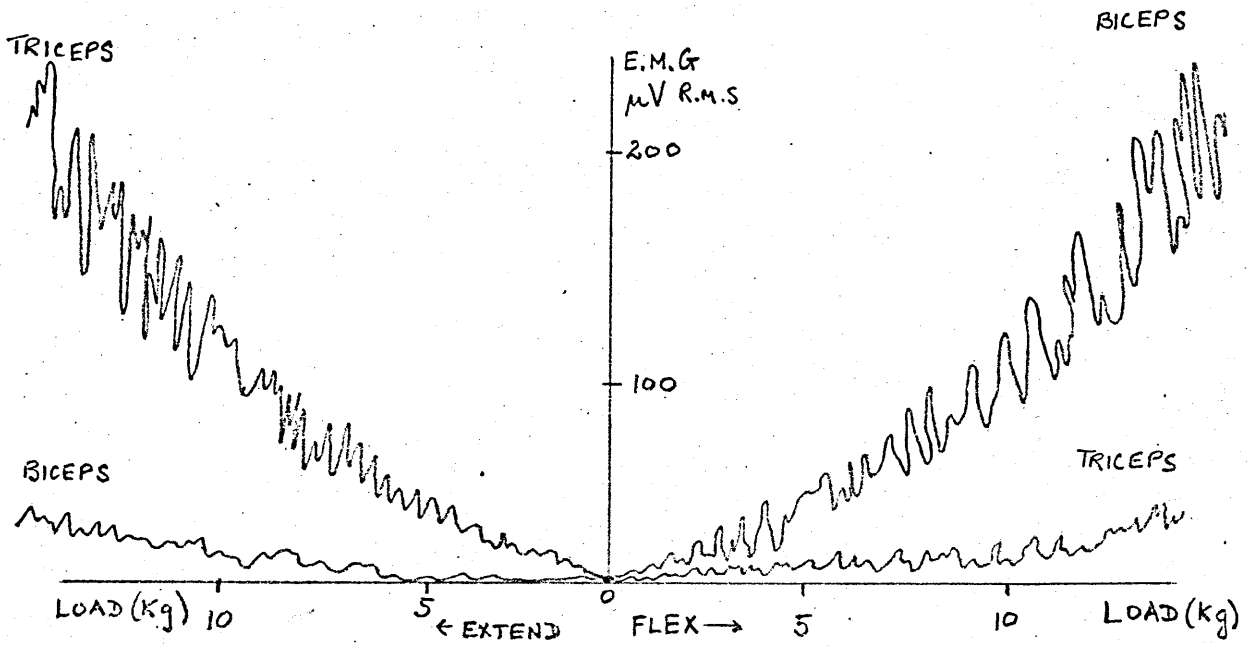


FIG. 4-5 RELATION BETWEEN E.M.G. AND LOAD APPLIED AT RIGHT ANGLES TO WRIST. ANGLE OF FLEXION 135 deg.

5. The control system

5.1 System consideration

A control system is to be attempted for a force-sensing elbow prosthesis. The completed device is shown in fig.5.11 .

The detailed description of a stepping motor is given in section 6 . In order to explain the reasoning behind the development of the control system it will be sufficient to say that the stepping motor can be operated from a train of pulses connected to either one of two inputs, one for clock-wise rotation, the other for counter-clockwise rotation.

The initial system considered is shown in fig.5.12. The mean pulse repetition frequency of the amplified E.M.G. signal is fed directly into one of the motor inputs. The completed device is to be force-sensing and hence force feedback is used. This force feedback voltage is to be used to control a gating circuit which prevents any pulses reaching the motor whenever the input and feedback pulse repetition frequency are equal.

Owing to difficulties experienced in designing the gating circuit, the system was modified to fig.5.13. Only one of the muscle pair - (the biceps) is now used and bi-directional motion should be obtained with this single input pulse train.



FIG. 5-11 THE COMPLETED PROSTHESIS.

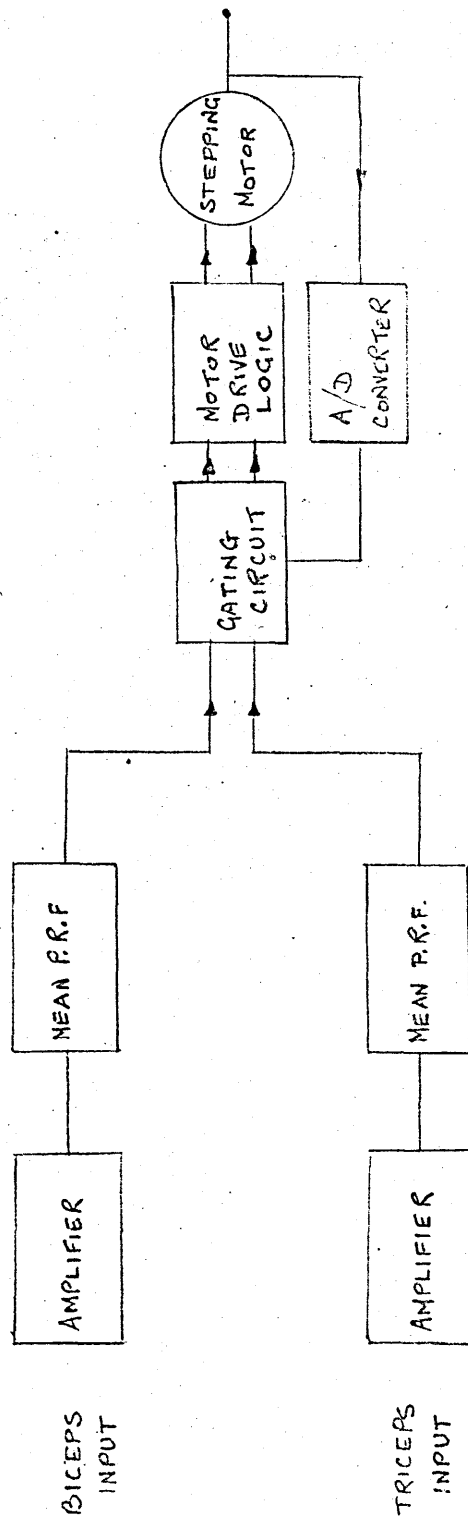


FIG. 5-12 INITIAL CONTROL SYSTEM.

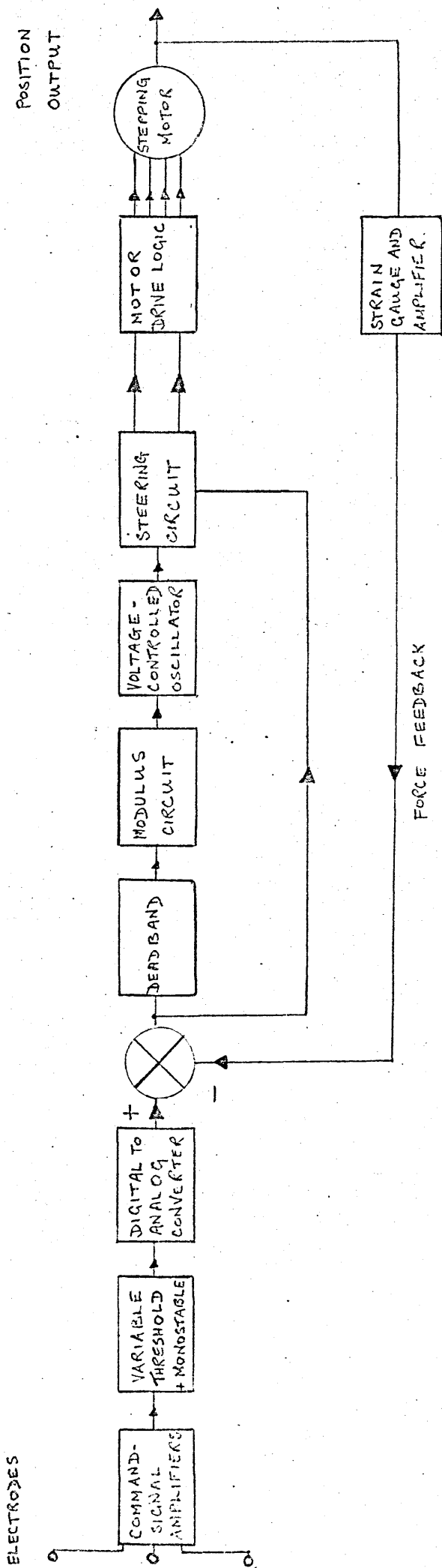


FIG. 5.2 THE COMPLETE CONTROL SYSTEM

## 5.2 Description of the complete control system

The E.M.G. signal is amplified and passed through a variable threshold. This enables variation in the level at which the E.M.G. signal triggers the monostable. This variable threshold can be used to obtain optimum performance. The maximum pulse repetition frequency is about 1000 p/sec., and hence the monostable period is set at less than  $\frac{1}{2}$  m.sec. The period chosen was  $\frac{1}{5}$  sec.

It is now necessary to obtain a dc voltage proportional to the p.r.f. of the signal. This is accomplished by means of a digital to analog converter. The diode in the smoothing circuit permits almost instantaneous response in output voltage for movement of the device in an upward direction. The downward direction has a slower response. The input voltage from the signals and the voltage feedback from the strain gauge amplifiers are fed to a difference amplifier. The output from this amplifier is then fed to the V.C.O by means of a dead-band and modulus circuit. The modulus circuit ensures that a positive voltage is always fed to the V.C.O. whether the difference amplifier output is positive or negative.

The difference amplifier output is also taken to a steering circuit whose operation is such that whenever an error exists at the output of the summing amplifier, the pulse train output from the V.C.O. triggers the motor logic in such a way that the error is reduced

5.3

E.M.G. SIGNAL AMPLIFIERS

Specification

- 1. Gain  
Variable between about 40 to 60 dB.
- 2. Bandwidth  
Approximately 10 Hz to 5 KHz
- 3. Common mode rejection ratio  
About 60 dB with 5 K $\Omega$  source imbalance.
- 4. Input impedance  
About 2 M $\Omega$
- 5. Low Noise

Design considerations

The input common mode rejection ratio (C.M.R.R.) of a differential amplifier is very dependent on the balance of the source impedances. For amplifier 3 in fig 5-1 the C.M.R.R. (s) is given by:

$$\frac{1}{S} = \frac{1}{H} + \frac{1}{S_A} \quad (1)$$

where  $S_A$  is the C.M.R.R. of the  $\mu 702c$  and  $H$  is the rejection factor of the external resistance bridge given by:

$$H = \frac{R_1 + R_2}{R_1} \frac{2}{\frac{R_1 - R_5}{R_5} - \frac{R_2 - R_3}{R_3}} \quad (2)$$

When the source resistances are added to  $R_1$  and  $R_5$  any imbalance will affect (1). This problem can be overcome by using the low output impedance of a  $\mu 702c$  to feed this differential amplifier. From appendix 1 the output impedance of amplifiers 1 and 2 is given by:



$$\frac{R_o}{1+A\left(\frac{2.5}{35 + R_5/10^3}\right)}$$

A high input impedance is achieved in amplifiers 1 and 2, by employing a 'bootstrapped' configuration giving positive feedback from the output to the non-inverting input pin (3). R<sub>3</sub> provides some thermal stability and is given by R<sub>3</sub> + R<sub>1</sub> ≈ R<sub>2</sub>.

The approximate expression for the input impedance of amplifier 1 is:

$$R_{in} = \frac{A R_a R_1}{(R_1 + R_2)} \quad (3)$$

where R<sub>a</sub> = input impedance of μ702c

A = open loop voltage gain of μ702c.

Using the maximum and minimum values of A and R<sub>a</sub> from the μ702c data sheet (appendix ) then:

$$R_{in} \text{ (max)} = 20 \text{ M}\Omega \text{ approx.}$$

$$R_{in} \text{ (min)} = 2 \text{ M}\Omega \text{ approx.}$$

The gain of this amplifier is given by:

$$\frac{R'_1 + R'_2}{R'_1} = 10$$

The setting up of the amplifiers for maximum C.M.R.R. is done as follows:

With a common signal applied to the inputs of amplifier 1 and 2 and observing the output from amplifier 3, the gains of amplifiers 1 and 2 are adjusted to give minimum output. The 5K potentiometer and 50K potentiometer in amplifier 3 are then adjusted to further minimise the output. Appendix 2 shows that there is little change in the output impedance for a 10K source resistance imbalance.

The results found in practice are given in table . The significant reduction in C.M.R.R. is due to the fact that the input impedance of 1 and 2 is not high enough. Photograph 4 shows a typical E.M.G. waveform obtained from the amplifiers constructed.

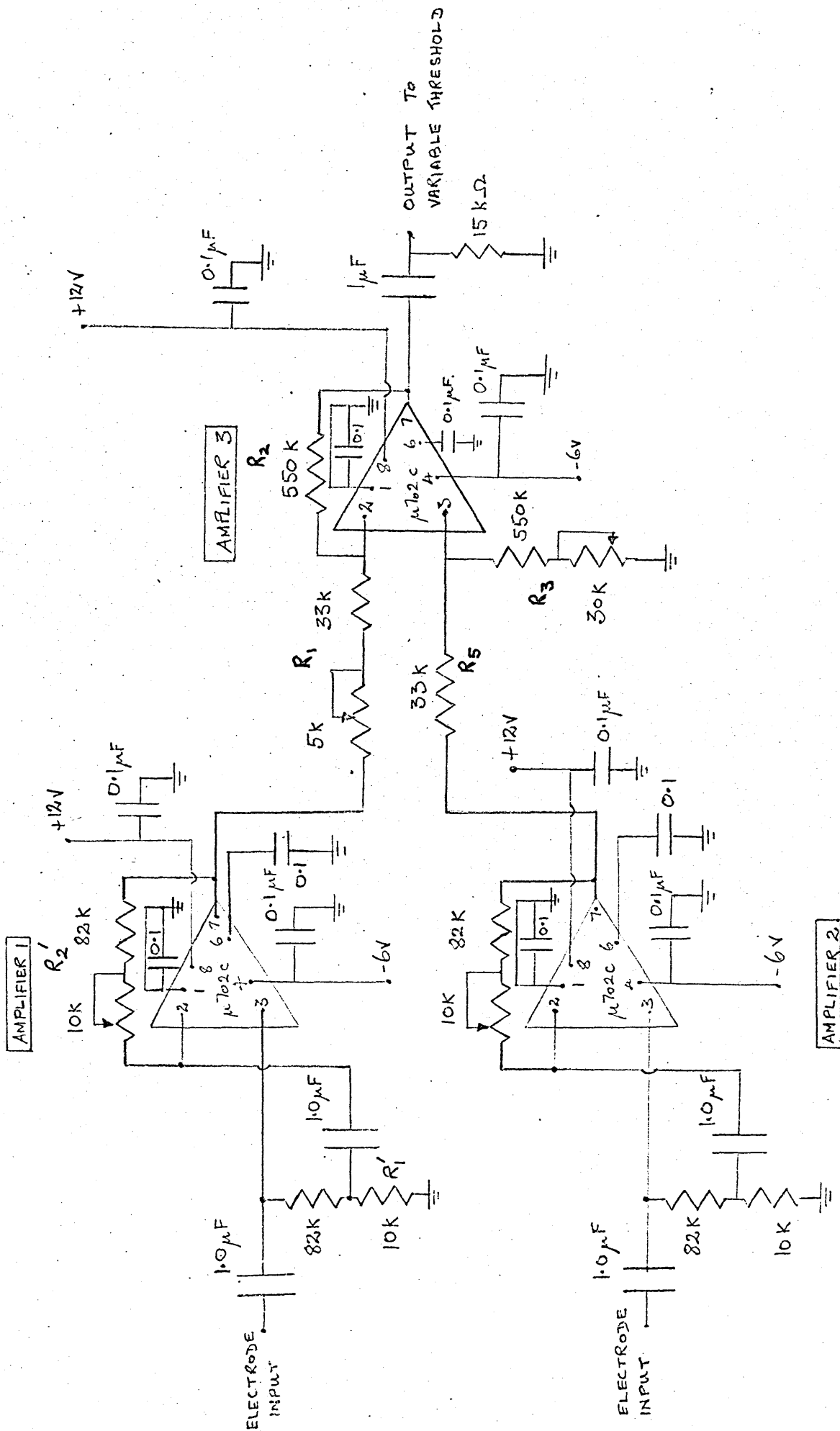


FIG. 5-31 E.M.G. SIGNAL AMPLIFIER

5.32 TABLE: E.M.G. SIGNAL AMPLIFIER RESULTS

Bandwidth:		30 Hz to 7 KHz			
C.M.R.R. $\cong$	Differential gain	Freq.	30 Hz	1 KHz	7 KHz
	Common mode gain		56 dB	64 dB	50 dB
C.M.R.R. with source imbalance at: 1KHz					
		Imbalance	C.M.R.R.		
		None	64 dB		
		5k	54 dB		
		10k	40 dB		
		100k	23 dB		

#### 5.4 Variable threshold and monostable circuit

A variable threshold is necessary to enable the comparator to be switched at a level above any noise present in the incoming signal. The circuit is shown in fig.5.4. The signal from the amplifiers is fed into pin 3 of the comparator. The threshold is set by varying the 250 $\Omega$  potentiometer. The comparator output switches between +3.1 v and -0.5 v accordingly as the input to pin 3 varies above or below the set threshold voltage appearing at pin 2.

The variable pulse width output is now converted into a constant pulse width by means of a monostable.

The maximum repetition rate of the incoming signal is about 1 KHz, a reasonable pulse width for the monostable would then be about  $\frac{1}{5}$  m. sec.

The monostable is triggered from the negative going edge of the comparator output. The monostable pulse width 't' is given by:

$$t = (R_s + R) C \log_e \frac{V_{out} R_s}{V_{ref} (R_s + R)}$$

where  $R_s$  = source resistance of  $V_{ref}$

$R$  = resistance for reducing recovery time.

$C$  = timing capacitor.

$V_{out}$  = output swing of  $\mu 710$  (= 3.6 volts).

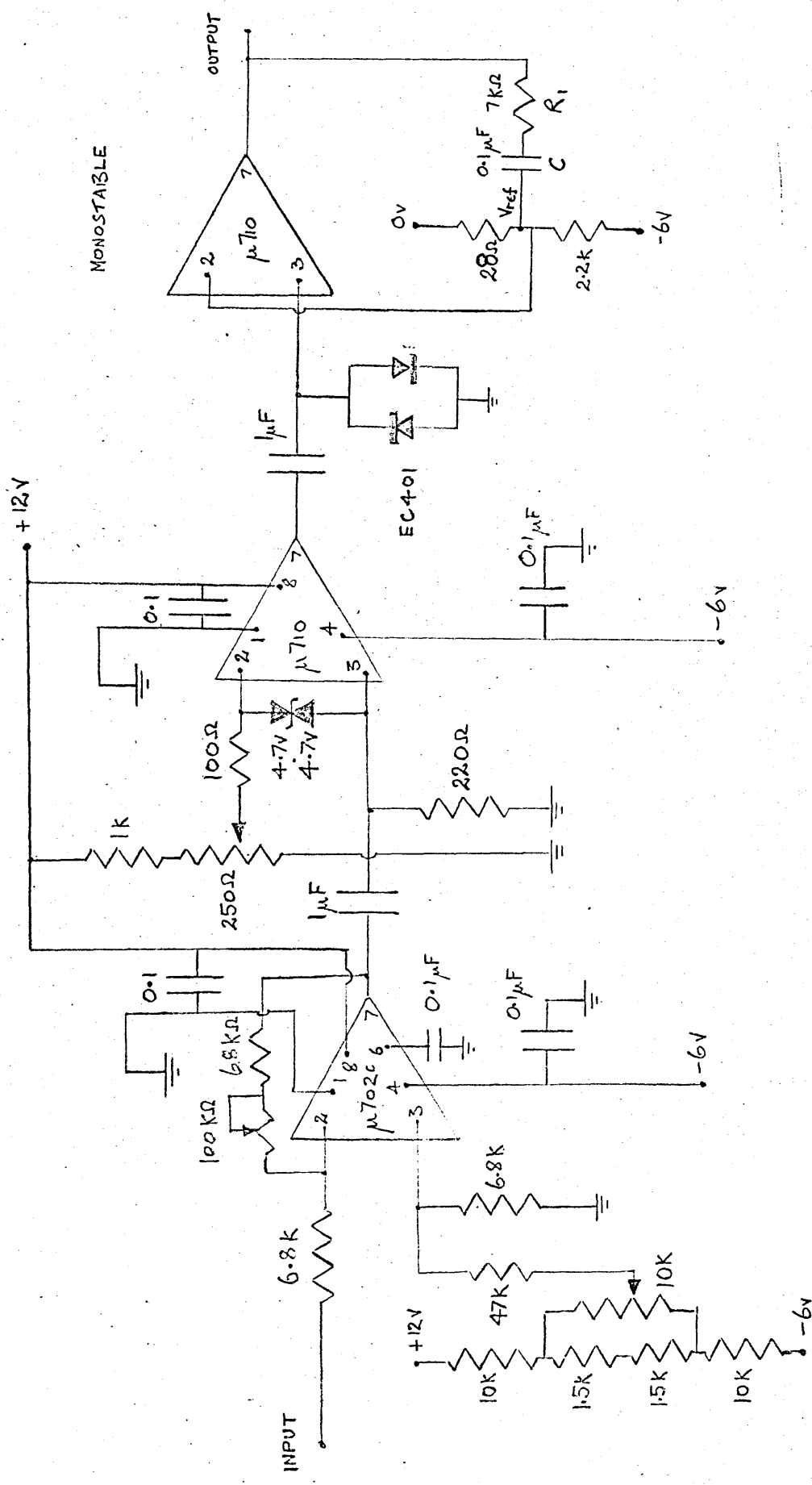


FIG. 5.4 VARIABLE THRESHOLD AND MONOSTABLE CIRCUIT

5.5 Digital/Analog converter

The D/A. converter fig.5-51 uses a Binary Coded Decimal counter, clocked by an astable multivibrator having a mark to space of 1 m.sec., and 10 m.sec. respectively.

During the 10 m.sec. 'space' the reset line to the counter is such that the input pulses are counted. The counter is reset to zero during the 1 m:sec 'mark' period.

The B.C.D. output is used to switch the transistors at the summing amplifier input. A staircase-shaped waveform appears at the output of this amplifier. This is then smoothed using a C.R. circuit and a 'fast attack' diode. The resistance is provided by the input resistance of the difference amplifier following.

The characteristic obtained for a 0.2 m.sec., input pulse width is given in fig.5-52. The ripple obtained on the d.c. output was about 0.2 volt.

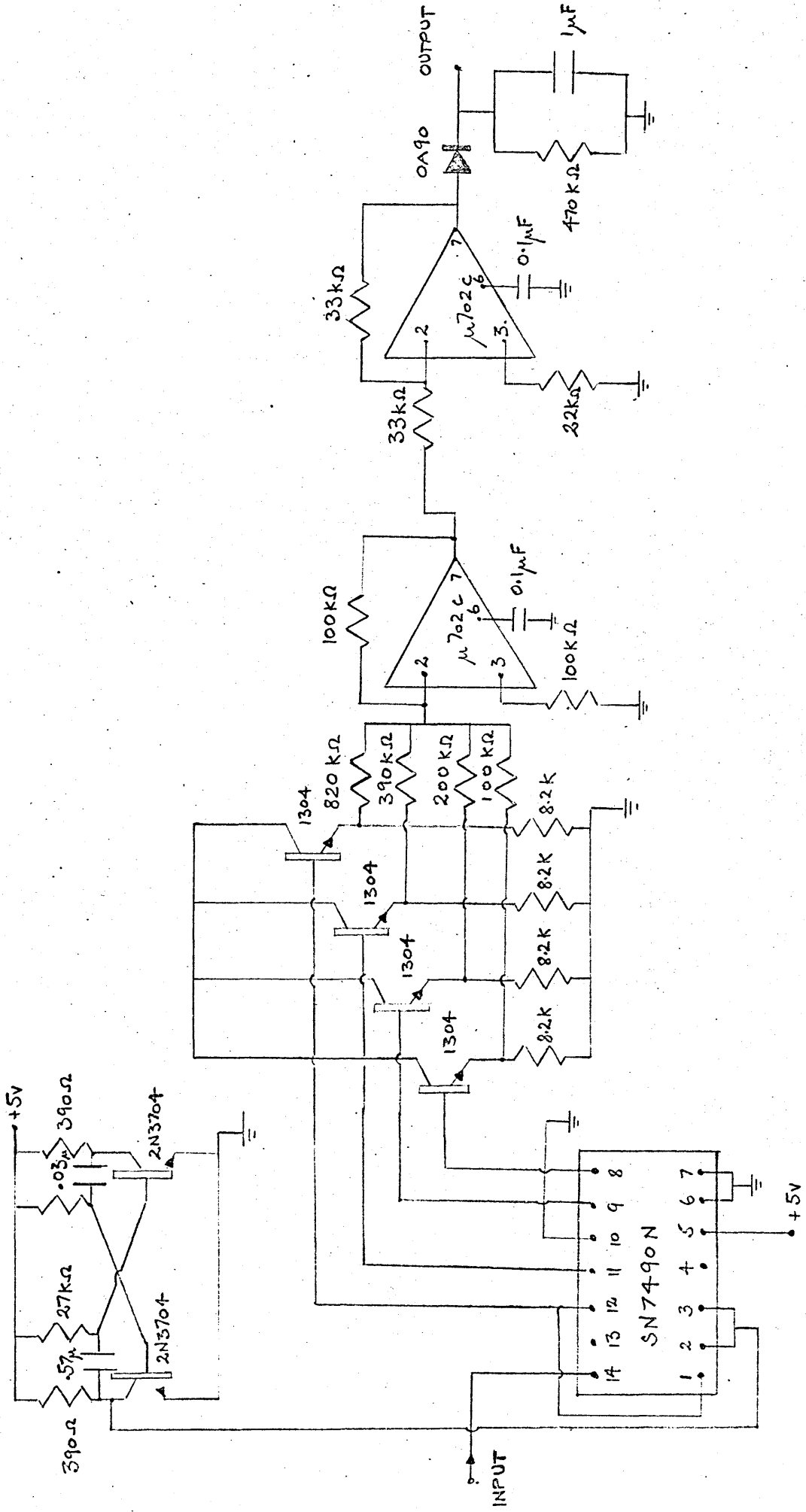


FIG. 5-51 DIGITAL TO ANALOG CONVERTER

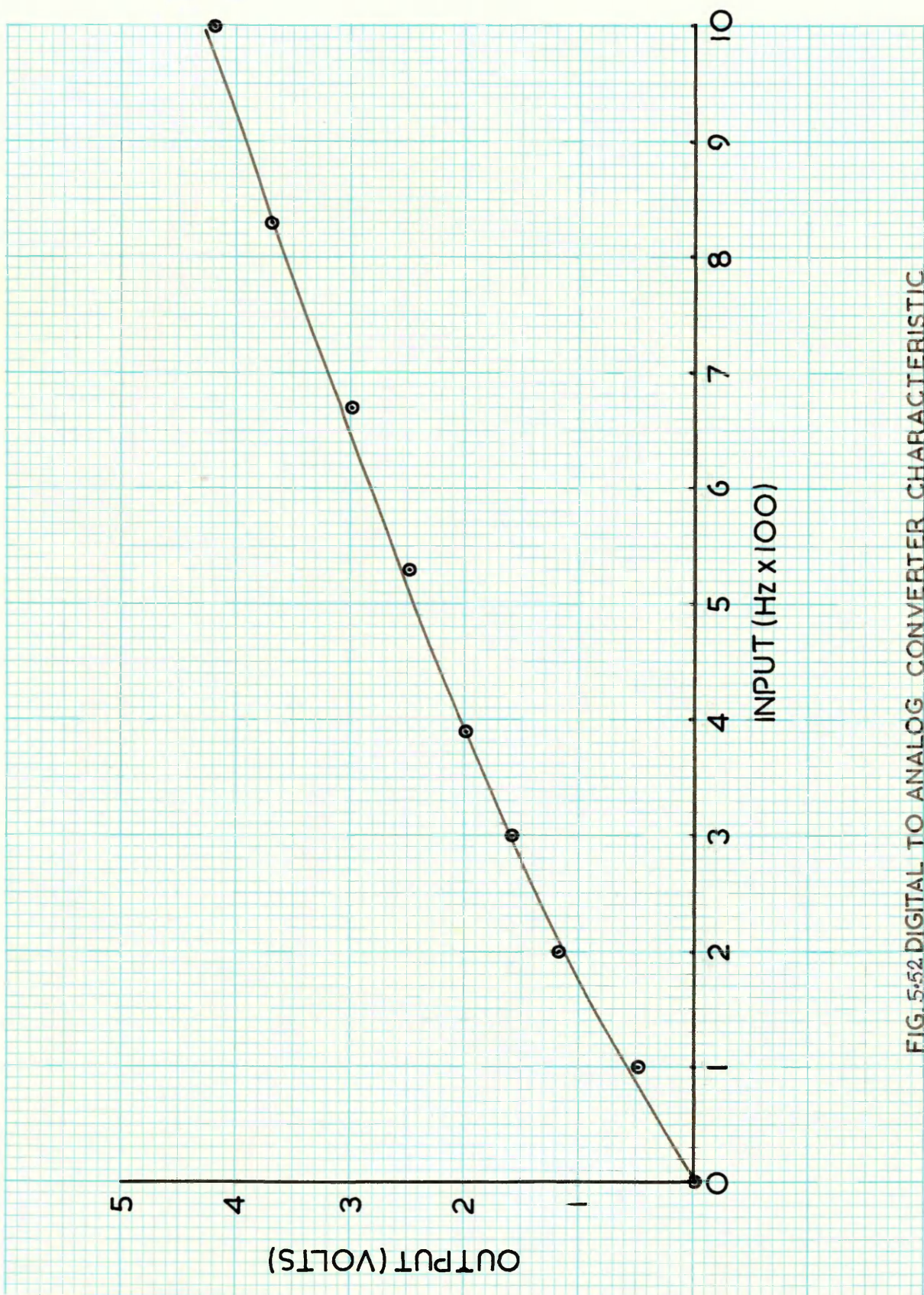


FIG. 5.52 DIGITAL TO ANALOG CONVERTER CHARACTERISTIC



## 5.6 Deadband and modulus circuit

The modulus circuit is given in fig.5.6 and its transfer characteristic is shown in fig.5.62.

The first integrated circuit amplifier acts as a unity gain half-wave rectifier giving a negative output for a positive input. The output from here is then fed together with the original signal into pin 2 of the second amplifier which acts as a summing amplifier via  $R_6$  and  $R_{10}$ . Because of the ratios  $R_8/R_{10}$  and  $R_8/R_6$ , the second amplifier operates with unity gain to the original signal and times two for the half-wave output signal.

The net effect is that the output is always positive-going and gives the absolute value of the input. This results from the fact that the negative input voltage is directly connected into the summing amplifier through  $R_{10}$ , whilst the half-wave output is zero.

The resistors  $R_3$  and  $R_7$  provide thermal stability and minimise the offset voltage.

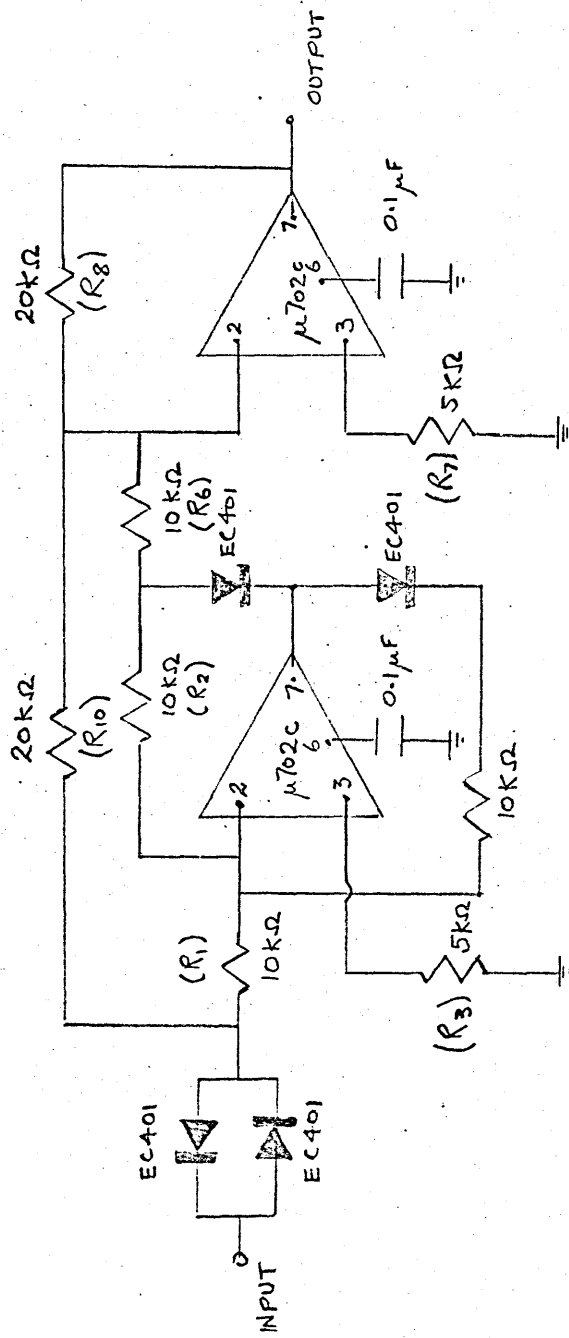


FIG. 5.61 DEADBAND AND MODULUS CIRCUIT

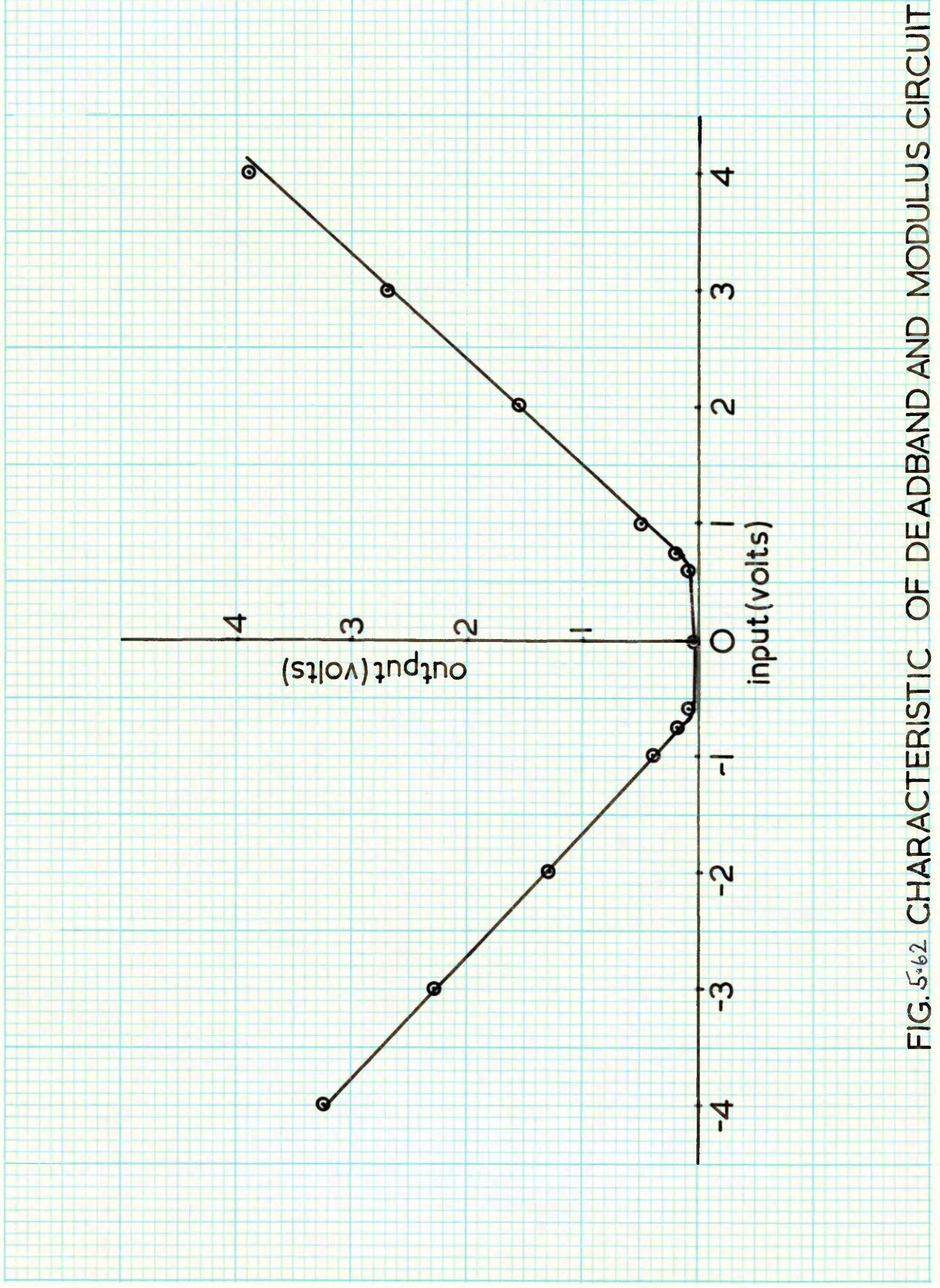


FIG. 5.62 CHARACTERISTIC OF DEADBAND AND MODULUS CIRCUIT

## 5.7 The voltage - controlled oscillator

The circuit shown in fig.5.71 is essentially a version of the conventional astable multivibrator, in which  $T_1$  and  $T_2$  are the main oscillator transistors. To ensure linear charging of the timing capacitors the two charging resistors are replaced by the transistor current sources,  $T_3$  and  $T_4$ . Transistors  $T_5$  and  $T_6$  are emitter followers for discharging the timing capacitors.

### Frequency sensitivity

The frequency sensitivity (S) is given by: (appendix 2).

$$S = \frac{1}{2 CRV_z}$$

With  $C = .068 \mu F$

$$S = 233 \text{ Hz/volt}$$

This value is chosen since the maximum output swing of the 702c is approximately 5 volts and the maximum motor pulse-rate input is approximately 1 KHz. The characteristic obtained is shown in fig. where the sensitivity is: 250 Hz/volt.

INPUT FROM MODULUS CIRCUIT

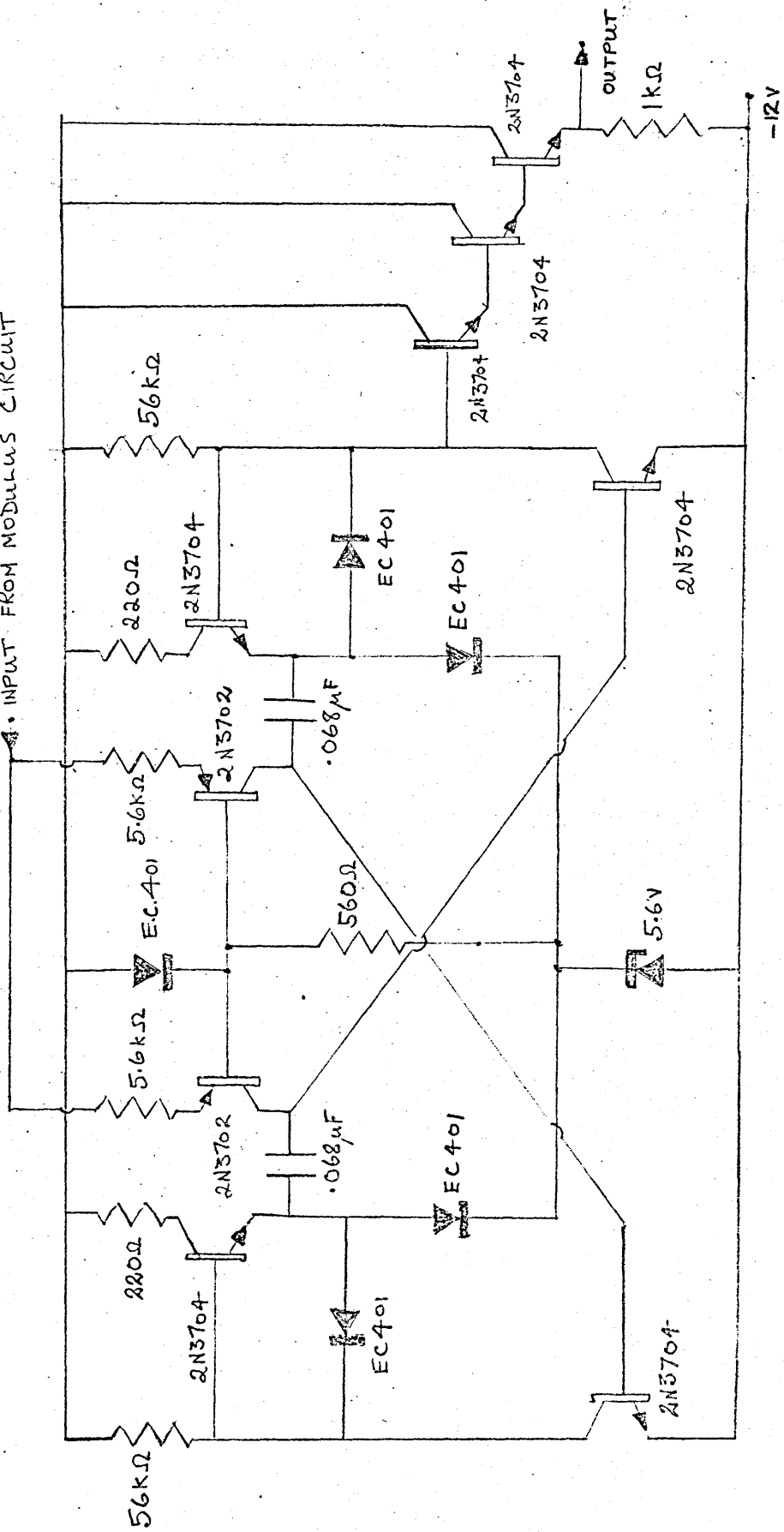


FIG. 5-71 VOLTAGE-CONTROLLED OSCILLATOR



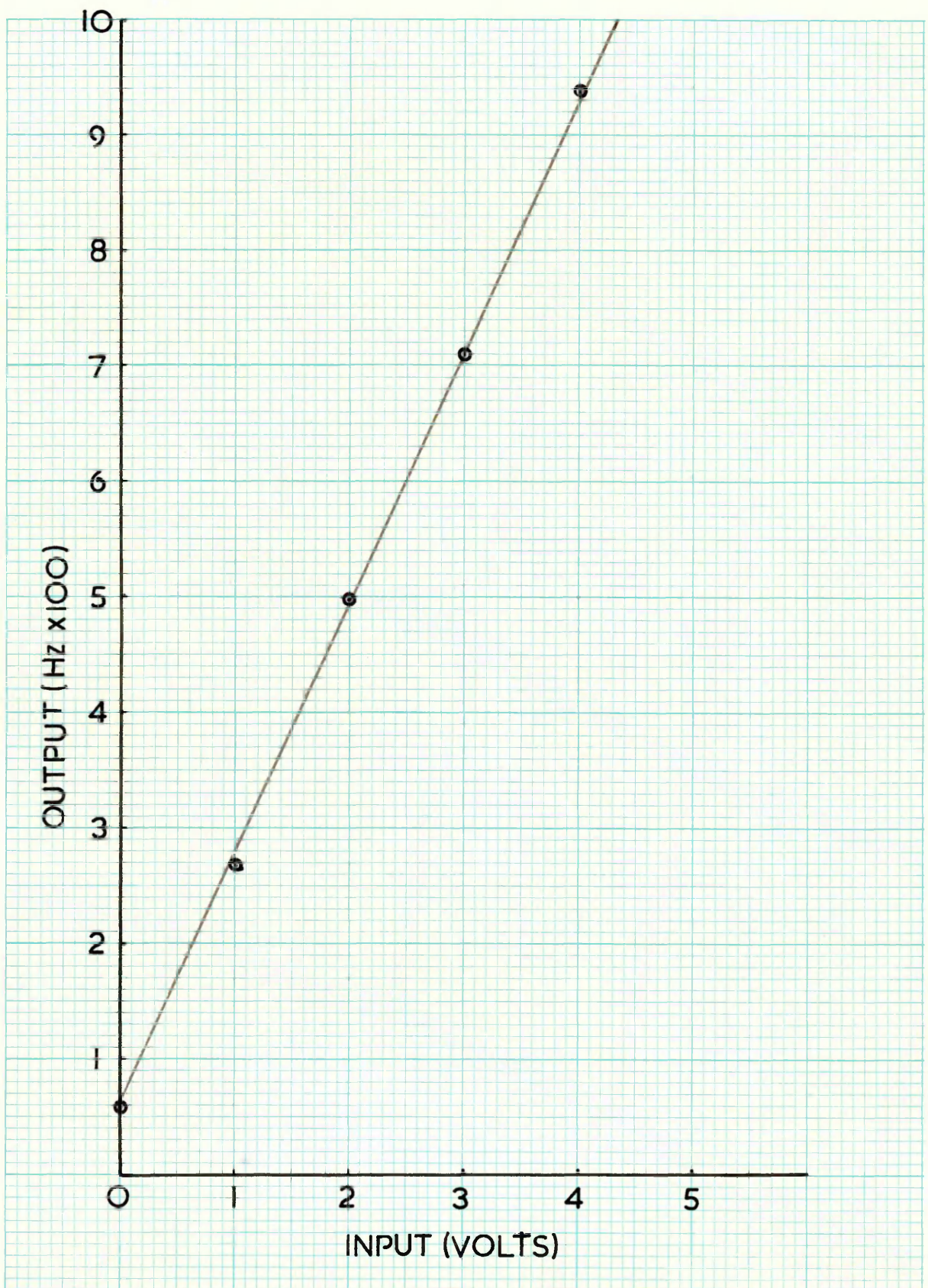


FIG.5-72 VOLTAGE-CONTROLLED OSCILLATOR CHARACTERISTIC

## 5.8 The steering circuit

The difference amplifier output is fed to a diode limiter and a  $\times 15$  amplifier as shown in fig.5.8 . The output of this amplifier is thus limited to about  $+ 5$  or  $- 5$  volts.

Hence with an error at the input to the difference amplifier, the output of the second amplifier will be about  $\pm 5$  volts. When no error exists at the input of the difference amplifier, then the output from the second amplifier will be zero.

With point A of the diode steering circuit at a positive voltage, the lower diode is brought into conduction, and the pulse train from the V.C.O. appears at output 1. With A negative, the pulse train appears at output 2. These two outputs are taken to the appropriate input of the logic drive so as to ensure closure of the loop.

This diode steering circuit also overcomes the problem of offset with the V.C.O. where a pulse rate output is present with the input voltage zero. With point A at ground, both sets of diodes are held off and hence no pulses are able to pass through either arm of the steering network.

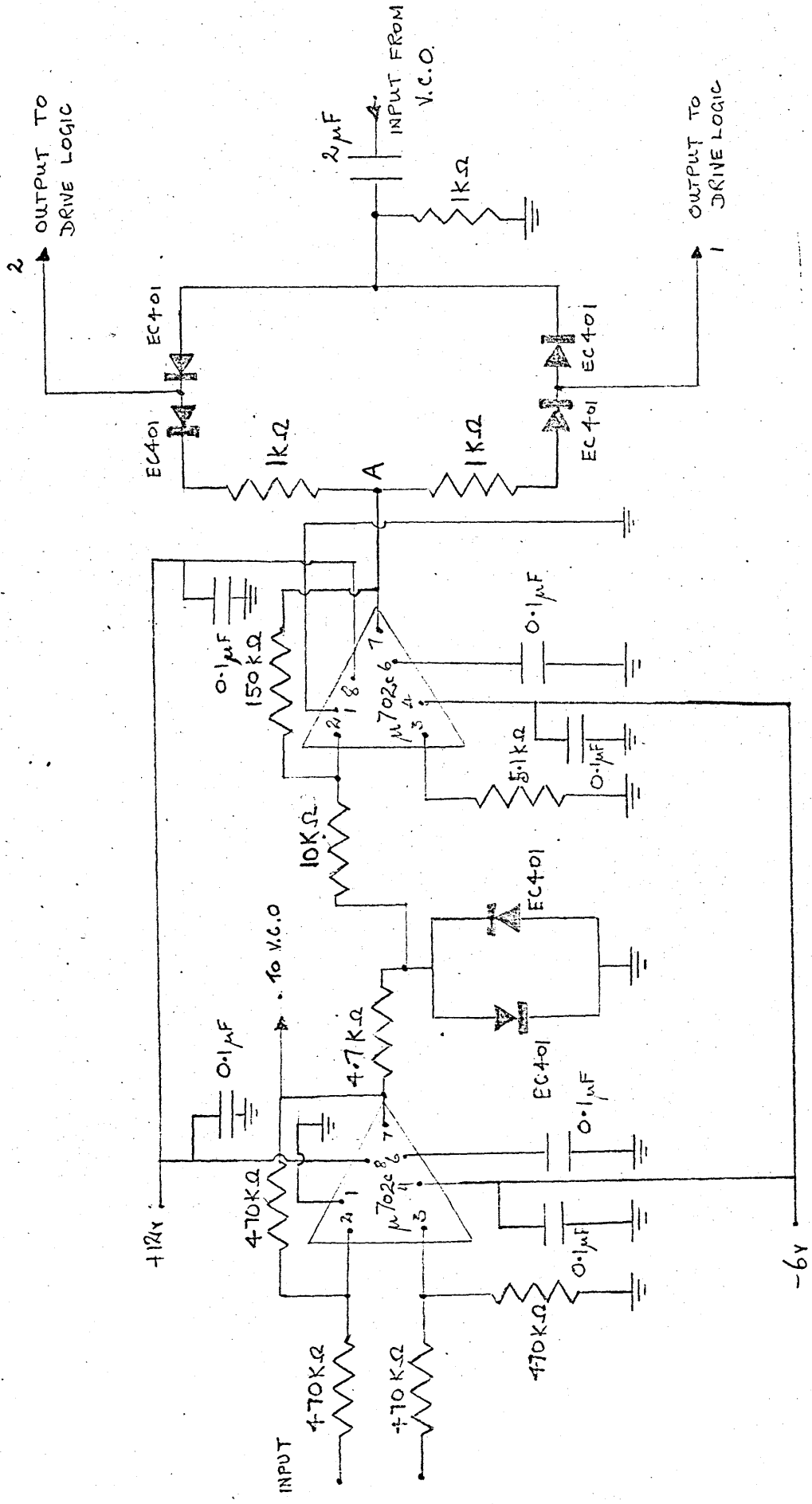


FIG. 5.8 STEERING CIRCUIT



## 5.9 Strain gauge bridge amplifier

The circuit is shown in fig 5.9 . The overall gain is variable between 60 and 75 dB (appendix 3 ). The 1K and 100K potentiometers in the input circuit of the first amplifier enable adjustment to be made for maximum input common mode rejection. The offset present at the output of the amplifier can be eliminated by adjusting  $R_{v1}$  and  $R_{v2}$ .

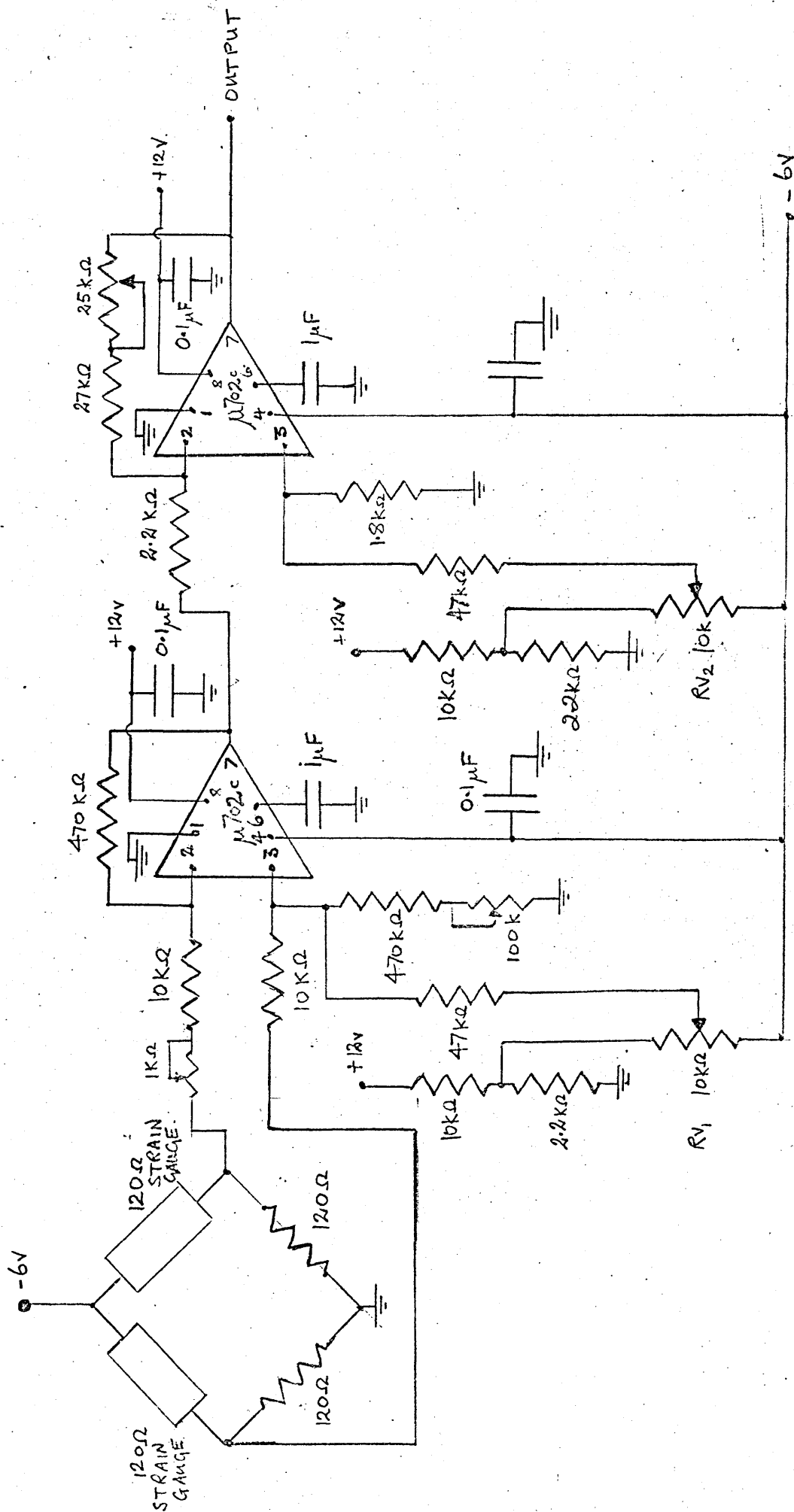


FIG. 5.9 STRAIN GAUGE BRIDGE AMPLIFIER

## 6. Actuator

### 6.1 Stepping motor operation

The stepping motor is, as its name suggests, a motor designed to rotate by a series of discrete steps rather than by continuous movement. The movement of the motor is based on the simple 'solenoid' electromagnet principle in which a ferromagnetic armature moves in the field of a coil carrying a current. This armature will move in such a direction that the flux linked with the exciting coil is increased.

Figure 6.1 (a) illustrates a motor with a four coil stator; 6.1(b), the switching sequence and the resultant stator field set up after each switching operation. The motor will follow this resultant stator field axis in order to achieve a position of maximum permanence, and will advance an incremental step equal to the vernier difference between stator and rotor pole pitch. Fig 6.1(c)

Between each switched operation, direct current passes through the stator coils and supplies a 'holding torque' which holds the rotor in the position to which it had been moved by the preceding switching operation.

### 6.2 Slo-Syn motor specification

The stepping motor chosen for this design is a 'Slo-Syn' motor type H.S. 25 manufactured by the Superior Electric Company U.S.A., and has the following specification:

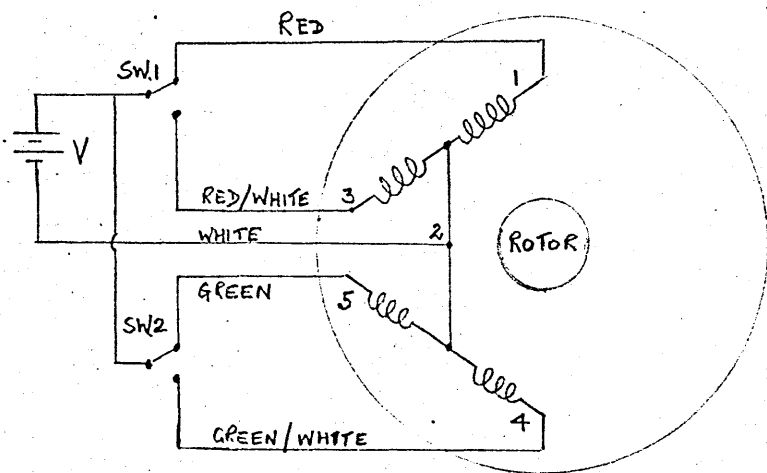
d.c. voltage	=	5.3v
Amps/winding	=	1.5
No. Steps/rev.	=	200
Maximum speed (Steps/sec)	=	1000 = 5 revs/sec.
Weight	=	2½ lb approximately.
Dimensions	=	3.25" by 1.86" diameter.
Starting torque	=	45 oz-ins.
'Holding' torque	=	58 oz-ins.

The torque/speed characteristics is shown in fig. 8 .

This motor was chosen because:

1. Its dimensions were suitable from a mechanical viewpoint.
2. Its weight was considered as being reasonable for the intended use.
3. The maximum pulse rate input acceptable to the motor is roughly the same as the maximum pulse rate of the command signal.

The holding torque of the motor should enable very simple mechanical locking in any position. This does however lead to a high wastage of power. To reduce this power wastage, it should be possible to reduce the motor current during a quiescent period.



STEP	SW1	SW2
1	1	5
2	1	4
3	3	4
4	3	5
1	1	5

FIG. 6.1(a) WIRING DETAILS OF MOTOR

FIG. 6.1(b) SWITCHING SEQUENCE

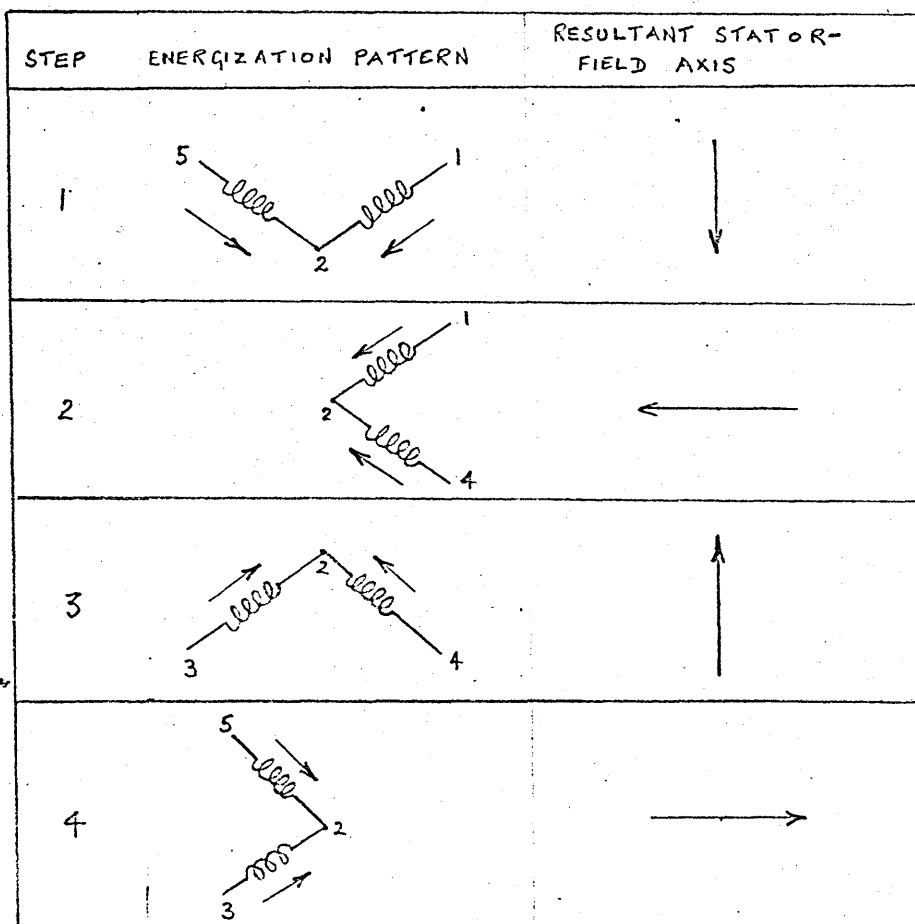


FIG. 6.1(c) RESULTANT STATOR FIELD

### 6.3 Stepping motor logic drive circuit

The switching sequence required for the correct operation of the H.S.25 stepping motor is shown in fig.6.31(b). This sequence is shown as a logic waveform in fig.6.31.

Such a sequence can be obtained from a pair of bistables with feedback arranged so as to form a 'switch tail ring counter'. This circuit is shown schematically in fig.6.32.

Reverse direction rotation is obtained by reversing the switching sequence.

The complete circuit is given in fig.6.33. The outputs from these bistables are taken to a power switch as shown in fig. 6.34

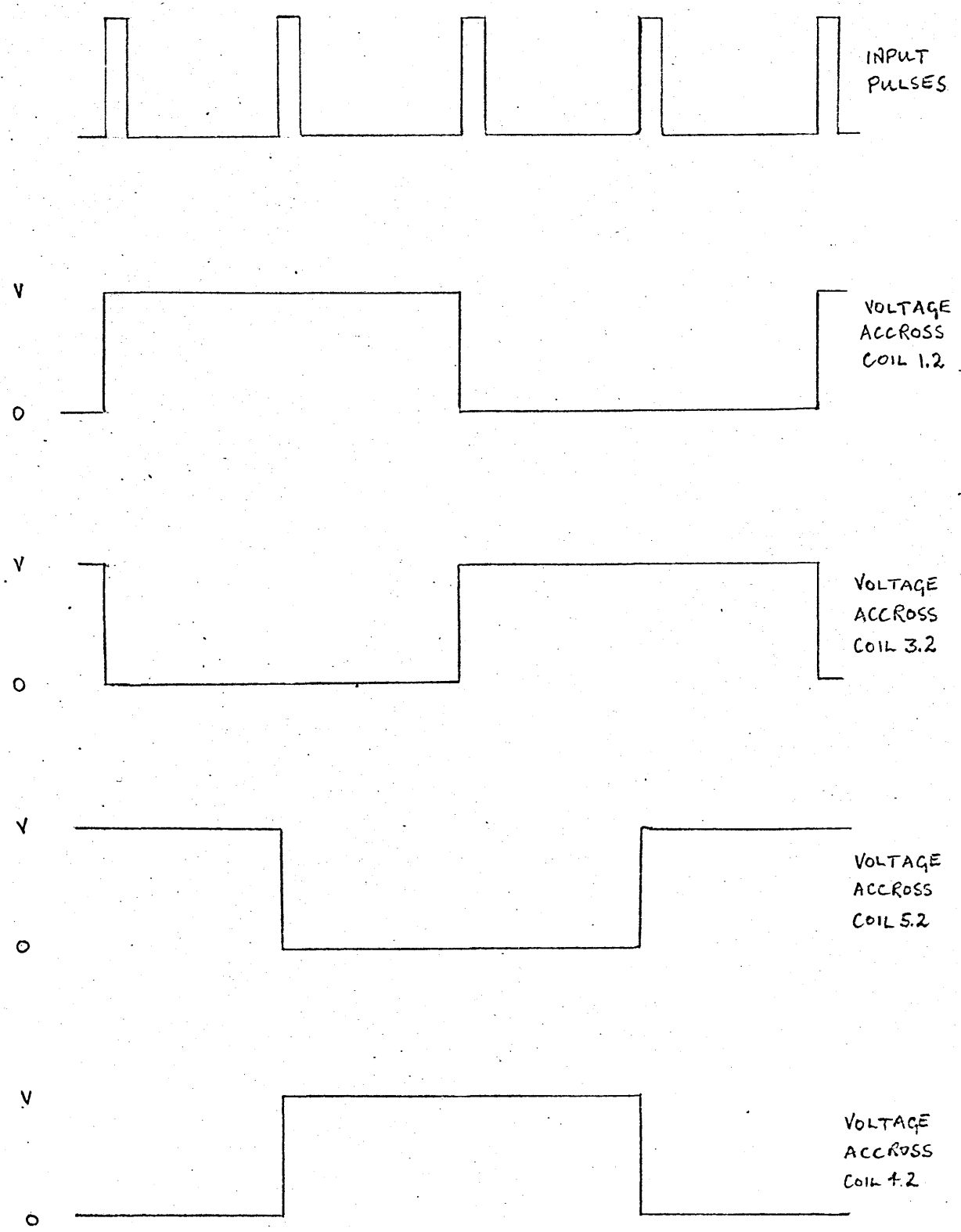
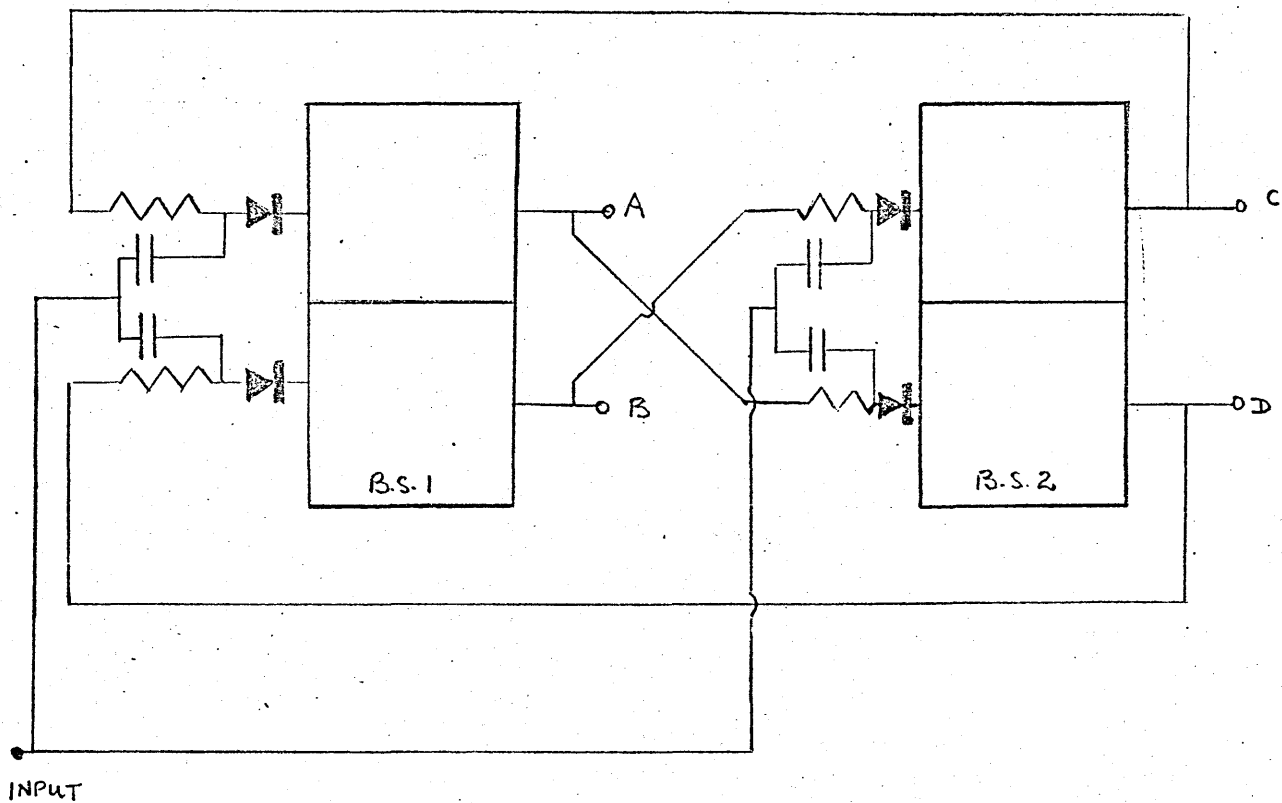


FIG. 6-31 LOGIC WAVEFORMS

CLOCKWISE ROTATION



COUNTER-CLOCKWISE ROTATION

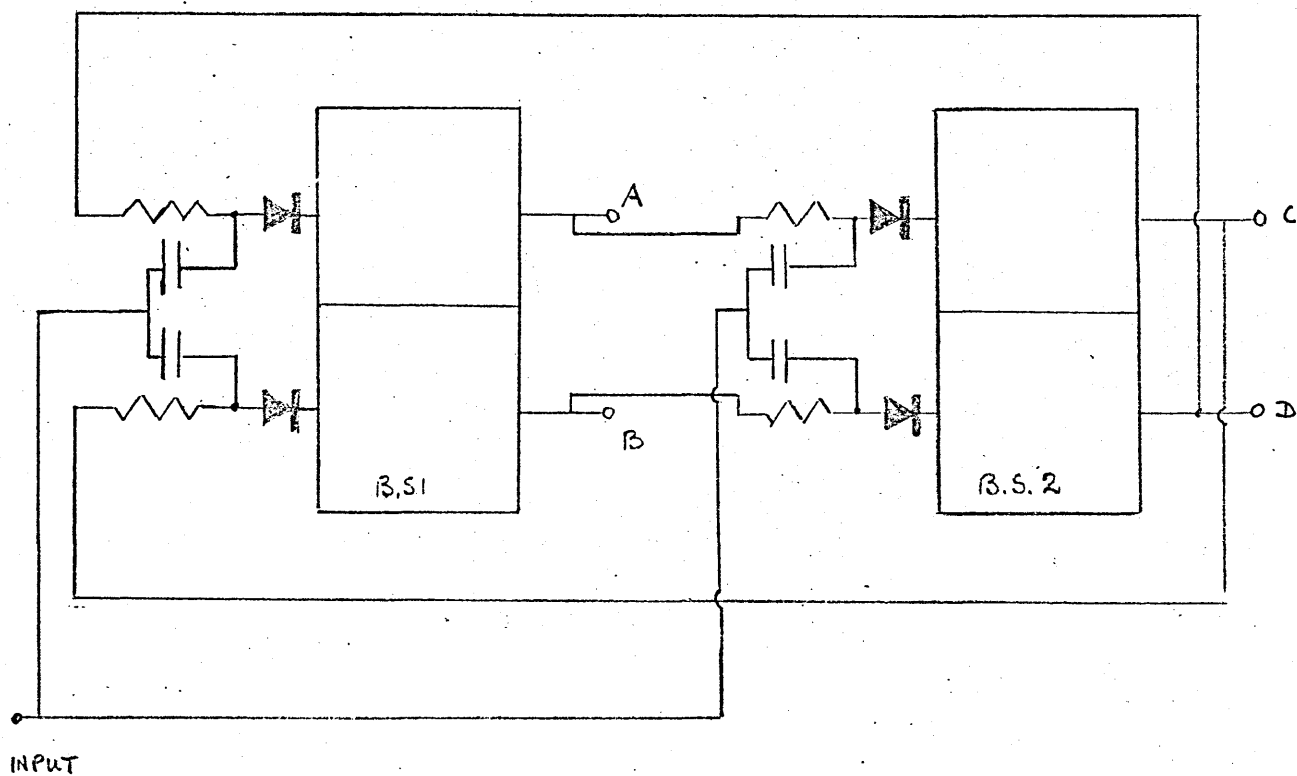


FIG. 6.32 SWITCH TAIL RING COUNTER



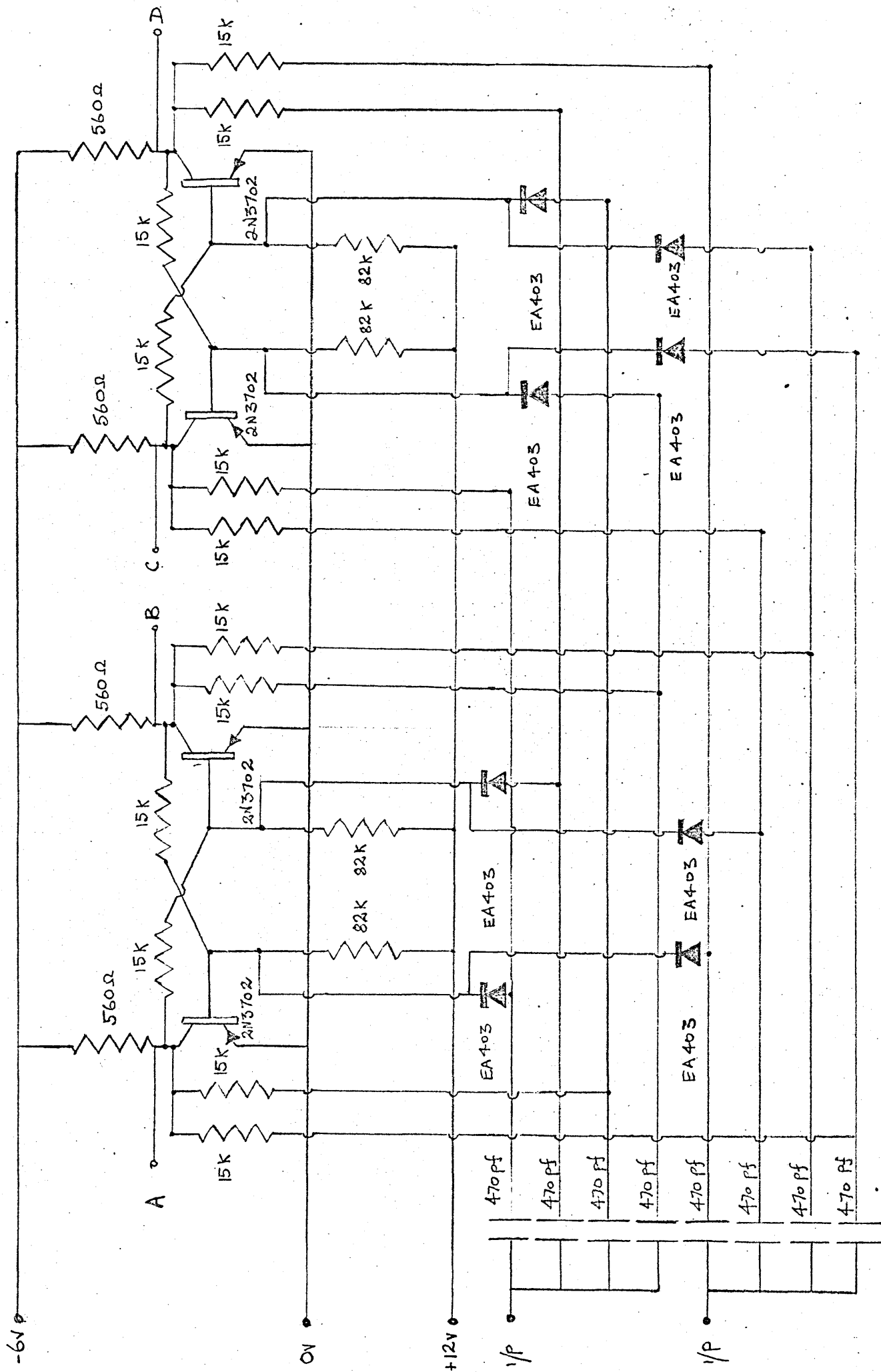


FIG. 6-33 MOTOR DRIVE LOGIC

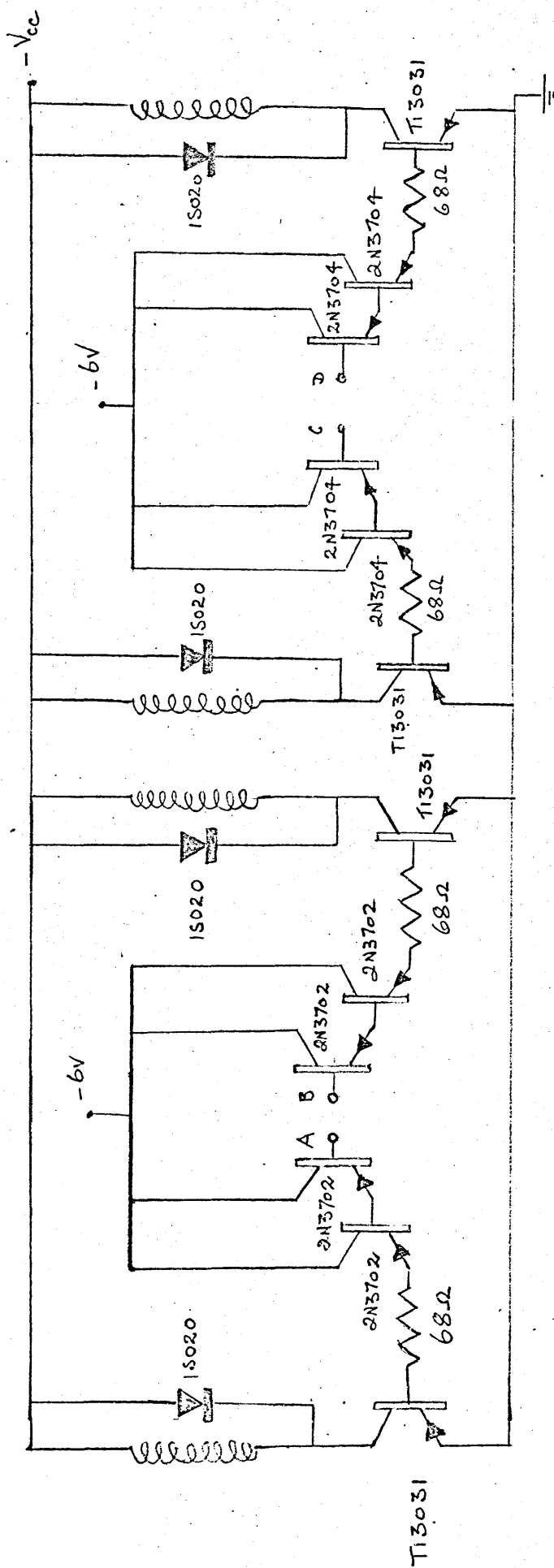


FIG. 6.34 POWER SWITCH FOR THE MOTOR DRIVE LOGIC

## 7. Mechanical Design

### 7.1 Mechanical specification

The prosthesis is to be designed for a short above elbow amputee and hence all the mechanical components must be incorporated in the forearm of the device.

1. Angle turned through by the forearm between  $10^{\circ}$  and  $135^{\circ}$  to the vertical.
2. Time of flexure over the complete range of movement about 5 secs.
3. Load - The device should be capable of lifting about one or two lbs. at a distance of 8 or 9 inches.
4. The device should be self-locking in any position.
5. It should be as light as possible.

### 7.2 Design consideration

The drawing of fig.7.21 shows the attempted design. The principle of the movement is based on the three bar linkage system. This simple system involves the shortening of a link which makes up one side of a triangle formed by three links.

The mass of the arm and that of the load cause flexure of the strut where strain gauges are fixed to provide a measure of the stress in the strut and, hence, a measure of the magnitude of the load. Calculations involving the strut are given in appendix 3 .

The photograph, fig.5.11, shows the motor and a threaded shaft forming this variable length link.

Fig.7.22 shows a close up of this shaft. The screw thread is semi-circular with a flat crest. This thread moves through a recirculating ball race giving the shaft/ball race unit an efficiency in the order of 95%.

When this unit was obtained from Rotax Ltd., it did

not possess the required pitch and shaft length. Consequently, as the motor had already been purchased the final performance regarding speed of flexure and angle of movement did not meet the specification.

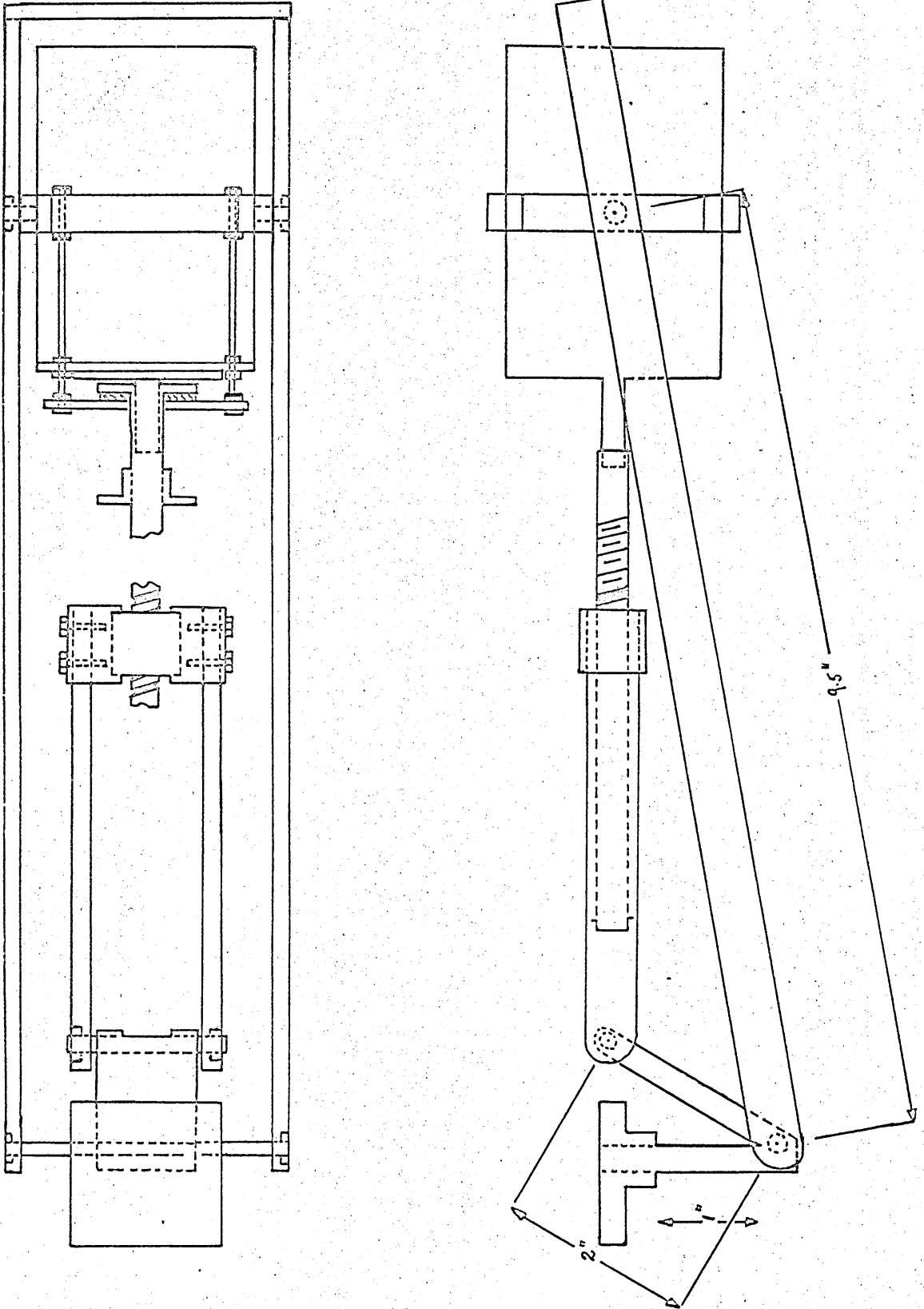


FIG. 7-21 MECHANICAL ASSEMBLY



FIG. 7-22 STEPPING MOTOR AND DRIVE SHAFT

## 8. Discussion

With a pulse generator supplying the input pulses to the control system, successful position control was obtained for various loads the angle of flexion being between  $30^{\circ}$  and  $135^{\circ}$  to the vertical. Mechanical locking was also achieved. Shortage of time prevented any stability assessments from being carried out. Direct drive from the biceps was also unable to be attempted.

Using a 20 volt supply for the motor and  $20\Omega$  in series with each stator coil, the minimum flexure time with a  $2\frac{1}{2}$  lb load was 18 seconds. (The long flexure time was obtained because the required screw pitch was unavailable). The current drawn from the 20 volt motor supply was approximately 1.5 amp. The motor was operating in an underated condition (Rated current 3 amp).

The resistances in series with the stator coils, together with an increased supply voltage above the rated 5.4 volts for the motor, is necessary in order to decrease the stator field current time-constant. The torque/speed characteristic for various time-constants is shown in fig. 8.

This series resistance results in a very serious wastage of power. As an estimate of the motor system's efficiency:

Supply voltage	=	=	20v
Supply current	=		1.5 amp (0.75 amp/winding)
Series resistance	=		$20\Omega$
Stator resistance	=		$\frac{5.4}{1.5} = 3.6\Omega$
Power supplied to motor	=		$20 \times 1.5$
	=		30 watts
Power dissipated in resistance	=		$4 \times 0.28 \times 23.6$
	=		26 watts
Efficiency	=		$\frac{4}{30} \times 100\%$
	=		13% approx.

Hence for this motor to be considered for use in a system requiring a high efficiency the following improvements must be made:

- (i). A means of decreasing the stator field current

time-constant without increasing the series resistance.

- (ii). A means of reducing the holding torque current during a quiescent period.



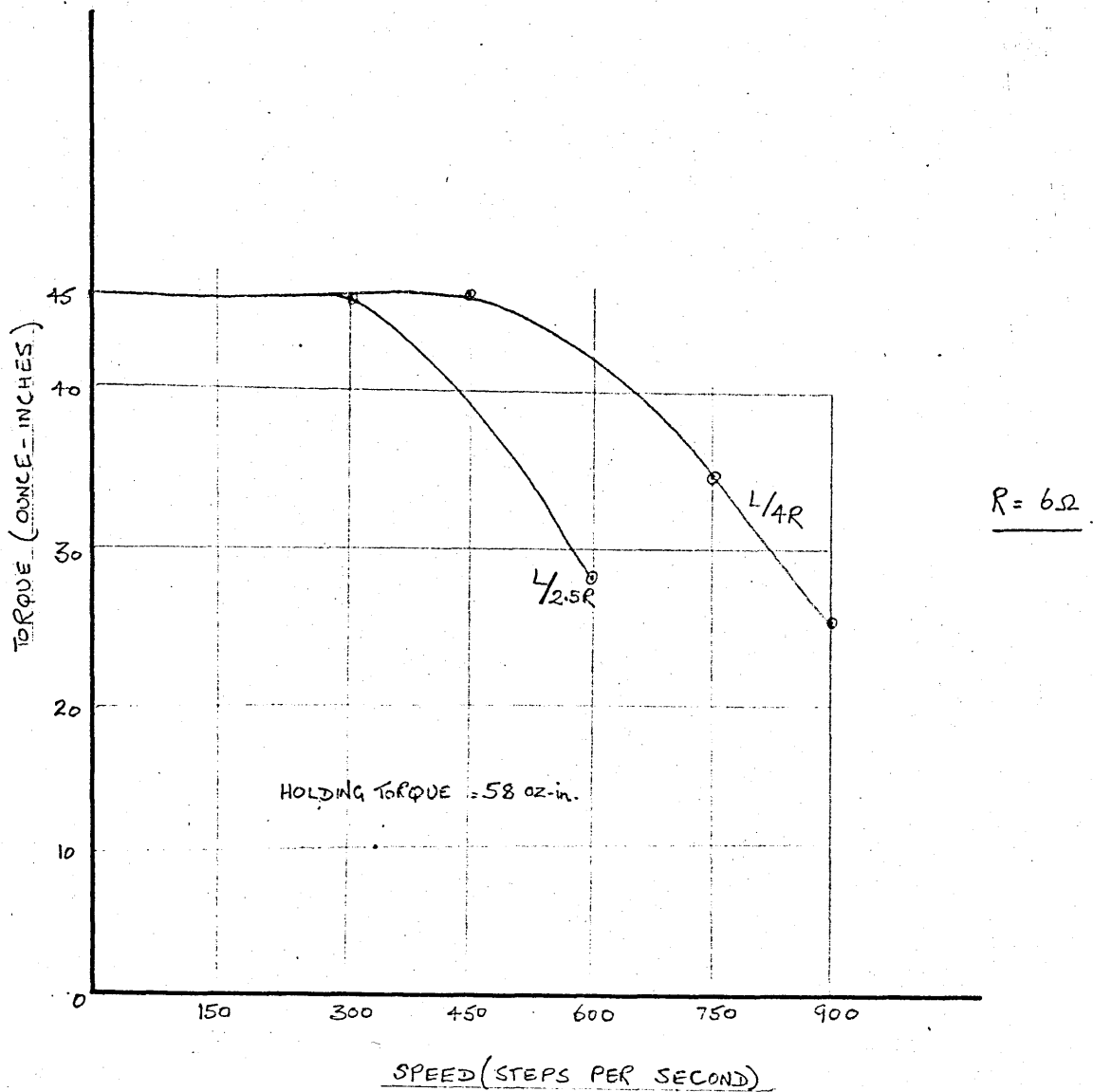


FIG. 8 TORQUE/SPEED CHARACTERISTIC OF H.S. 25  
 STEPPING MOTOR FOR DIFFERENT FIELD CURRENT  
 TIME CONSTANTS.

#### ACKNOWLEDGMENT

I would like to express my gratitude to my supervisor Mr. Thomason for his helpful suggestions; also to Mr. Dorell and Mr. Hemmings of the workshop, Dr. Lewes of Bedford Hospital and Messrs Rotax Ltd. for supplying the recirculating ball race and screw.

## REFERENCES

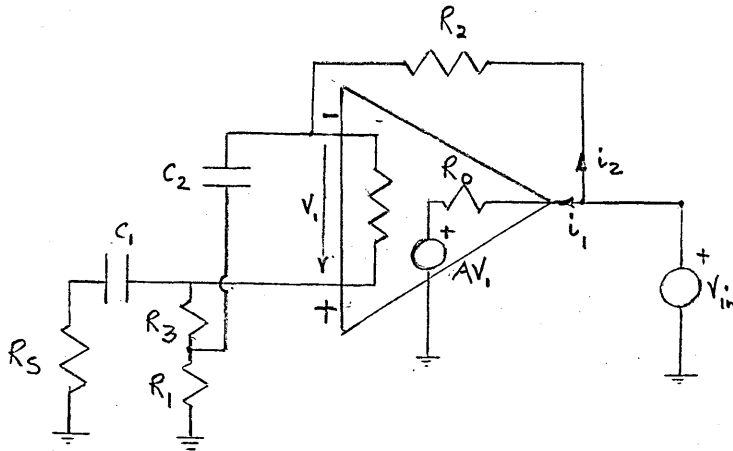
1. Professor G. Jentshura. Malformations and amputations of the upper extremity. Grune & Stratton Pub.
2. Dr. A.H. Bottomley. Artificial hand controlled by the nerves. New Scientist Vol. 21 pps 668-671.
3. A.K. Godden. Techniques of Myoelectric control of prosthesis and the prospect of this type of control for thalidomide casualties. Oxford Univ. Dept. Eng. Sc. Report.
4. Medical and Biological Eng. Vol.5 pps 111-125 1967.
5. E.M.G. Patterns at multiple muscle sources in the control of external power in Upper Extremity Rehabilitation. NAS-NRE Washington Pub. 1352, 1966.
6. Collecting the body's signals Electronics 103-112, July, 10, 1967.
7. Muscle spindles and their motor control. Physiol. Rev. 44 219
8. A. Bottomley. Muscle substitutes and myoelectric control. J. Brit.I.R.E. Vol. 26 No.6 Dec. 1963
9. Case Institute of Technology R & D Report No.5 Dec.1966 pps 35-52 'Medical Eng.'
10. An E.M.G. Controlled Force-Sensing Proportional Rate Elbow Prosthesis. M.I.T. Report.
11. An E.M.G. Operated Control System for a prosthesis Medical & Biol. Eng. Vol.5 pps. 597-601

- |     |                           |   |   |
|-----|---------------------------|---|---|
| 12. | M.J. Hall.                | Artificial limbs - a brief historical survey.   | University College, London<br>Report No.64/4.                       |
| 13. |                           | Myoelectric control systems progress.   | Reports Nos. 2,5,6 & 7.<br>Univ. of New Brunswick<br>Bio-Eng. Inst. |
| 14. | M.J. Hall,<br>T. Lambert. | On the use of muscle electric potential for the position control of artificial limbs. | Mech. Eng. Dept. Univ. College, London.                             |
| 15. |                           | Group on power and control systems for upper limb prostheses.                         | Progress Report No.1.   |
| 16. |                           | Proc. Symposium on powered prostheses   | Roehampton, 1965.   |
| 17. |                           | Strain gauge measurement concepts.  | Tektronix Inc.  |
| 18. | S.G.S. Fairchild.         | The application of linear micro-circuits.   |   |
| 19. |                           | Drive circuits for stepping motors  | Mullard Tech. Communications.<br>Vol.8, No.72<br>Sept. 1964.        |
| 20. | R.D. Middlebrook.         | Differential Amplifiers.  |   |
| 21. |                           | A transistorised pulse drive for a stepping motor.                                    | Electronic Eng. May, 1966.  |
| 22. |                           | Simple wideband linear voltage to frequency converter.                                | Electronic Eng. March, 1968.  |
| 23. |                           | Study of skin impedance.  | Electronics. April, 1950, pps 190-196.                              |

## APPENDICES

APPENDIX 1

Output impedance of bootstrapped amplifier.



- A = open loop voltage gain
- $R_{in}$  = input impedance of  $\mu 702c$
- $R_o$  = output impedance of  $\mu 702c$
- $R_s$  = source resistance.

Neglecting the reactances of capacitors  $C_1$  and  $C_2$ , the circuit can be redrawn as in fig. A1

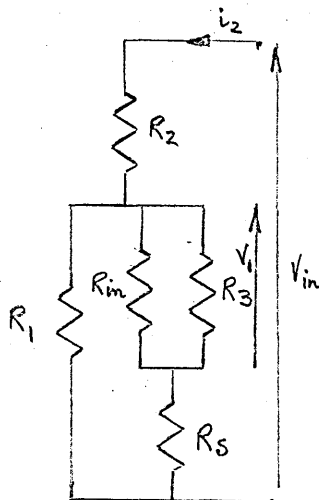


FIG. A1

$$\text{Voltage } V_1 = \left[ \frac{R_A R_1}{R_2(R_1 + R_A + R_S) + R_1(R_A + R_S)} \right] \cdot V_{in}$$

$$\text{where } R_A = \frac{R_{in} R_3}{R_{in} + R_3}$$

$$\text{With } R_{in} = 32K\Omega$$

$$R_3 = 82K\Omega$$

$$\text{then } R_A = 23K\Omega$$

$$\text{and } V_1 = \left[ \frac{2.5}{35 + R_S/10^3} \right] \cdot V_{in}$$

$$\text{Current } i_1 = \frac{V_{in}}{R_o} \left[ A \cdot \left( \frac{2.5}{35 + R_S/10^3} \right) + 1 \right]$$

and since  $i_2 \ll i_1$  then the output impedance is:

$$R_o^1 = \frac{V_{in}}{i_1} = \frac{R_o}{\left[ 1 + A \frac{2.5}{35 + R_S/10^3} \right]}$$

$$\text{For } R_S = 0$$

$$R_o^1 = 1.1\Omega$$

$$\text{For } R_S = 10K$$

$$R_o^1 = 0.8\Omega$$

APPENDIX 2

FREQUENCY SENSITIVITY OF V.C.O.

With reference to fig.

I = current provided by each of the two current sources

T = period of oscillation

C(=C<sub>1</sub>=C<sub>2</sub>) = timing capacitance

V<sub>z</sub> = zener voltage

Then I is given by

$$I = \frac{V_x - V_{eb}}{R} \quad (1)$$

where V<sub>x</sub> = control voltage

V<sub>eb</sub> = emitter base voltage of T<sub>3</sub> and T<sub>4</sub>

Neglecting the saturation voltage of either T<sub>1</sub> or T<sub>2</sub> in comparison with the zener voltage, then the voltage swing at either base of the oscillator transistors is equal to the zener voltage V<sub>z</sub> (Ref. 22).

Hence for a symmetrical circuit

$$I \frac{T}{2} = CV_z \quad (2)$$

Thus from (1) and (2) the frequency sensitivity (s) is:

$$S = \frac{1}{2 CRV_z} \text{ Hz/Volt}$$



## APPENDIX 3

### STRUT DESIGN

#### Measurement of bending strains

Fig.A3-1 shows the stress pattern produced within a beam upon application of a force.

It is necessary to determine if the physical dimensions and the type of material making up the transducer body can produce sufficient output at the lowest force of interest. It is also necessary to determine the dynamic range of the finished transducer. This is a function of the minimum usable output at one end and the maximum acceptable stress within the proportional limit at the other end.

Consider the cantilever with the dimensions given in fig. A3-2 and made of Aluminium-Magnesium Alloy (10% Mg.)

$$\text{Section Modulus } Z = \frac{WH^2}{6}$$

where  $W$  = width of beam

$H$  = height of beam

$$\text{Thus } Z = 1 \times \left(\frac{1}{4}\right)^2 \times \frac{1}{6} = \frac{1}{96} \quad (1)$$

Surface stress  $\sigma$  at gauge application point

$$\sigma = \frac{FL}{Z} \quad (2)$$

where  $F$  = Force

$L$  = length from loading point to centre of gauge area.

$$\text{Strain } (\epsilon) = \frac{\sigma}{E} \quad (3)$$

where  $E$  = Youngs Modulus

=  $(1.03 \times 10^7$  for the alloy used).

Thus, from equations (1), (2) and (3), it is possible to

determine the strain at the gauge application points.

It is now necessary to determine the maximum and minimum values of the bending moment.

From fig. A3.3 the maximum and minimum value of this moment will occur when the projection of OP on the horizontal is a maximum and minimum respectively.

$$\begin{aligned} \text{Hence } (F.L)_{\min} &= 9.5 \times W_1 \times \sin 30^\circ \\ \text{and } (F.L)_{\max} &= (9.5 \times W_1) + (13.3 \times W_L) \\ \text{where } W_1 &= \text{unloaded weight} = 3\frac{1}{4} \text{ lbs.} \\ W_L &= \text{load} \end{aligned}$$

The unloaded weight is assumed to act through the pivot at Q

For a 2 lb load

$$\begin{aligned} (F.L)_{\max} &= (9.5 \times 3.3) + (13.3 \times 2) \\ &= 57 \text{ lb-in} \\ \text{And } (F.L)_{\min} &= 9.5 \times \sin 30^\circ \times 3.3 \\ &= 15 \text{ lb-in} \end{aligned}$$

From equation (2)

Surface stress at gauge application point

$$\begin{aligned} \sigma_{(\max)} &= \frac{57}{1/96} = 5.47 \times 10^3 \text{ p.s.i} \\ \sigma_{(\min)} &= \frac{15}{1/96} = 1.4 \times 10^3 \text{ p.s.i} \end{aligned}$$

From equation (3) Strain  $\epsilon$  is given by

$$\begin{aligned}\epsilon_{(\max)} &= \frac{\sigma_{\max}}{E} \\ &= \frac{5.47 \times 10^3}{1.03 \times 10^7} \\ &= 521 \text{ micro inches/inch}\end{aligned}$$

And

$$\begin{aligned}\epsilon_{(\min)} &= \frac{1.4 \times 10^3}{1.03} \\ &= 140 \text{ micro inches/inch}\end{aligned}$$

The alloy used has a yield point of 25,000 p.s.i. i.e. a yield strain of  $\frac{25,000}{E}$  or 2,500 micro inches/inch

$E$

the maximum strain is therefore well within the limit.

Bridge output voltage ( $e_o$ )

$$e_o = \frac{\text{total strain} \times \text{bridge voltage} \times \text{gauge factor}}{4} \quad \text{volts}$$

Two gauges are used in such a manner as to double this voltage hence the bridge output voltage becomes

$$e_o = \frac{\text{total strain} \times \text{bridge voltage} \times \text{gauge factor}}{2}$$

$$\begin{aligned}\text{And } e_o \text{ max} &= \frac{521 \times 6 \times 2}{2} \\ &= 3.1 \text{ mV approx.}\end{aligned}$$

$$\begin{aligned}e_o \text{ min} &= \frac{140 \times 6 \times 2}{2} \\ &= 0.8 \text{ mV}\end{aligned}$$

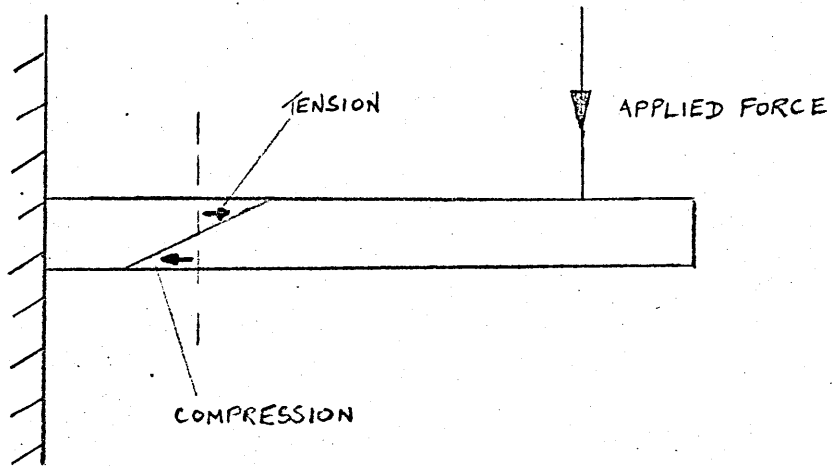


FIG. A 3:1 STRESS PATTERN IN A CANTILEVER

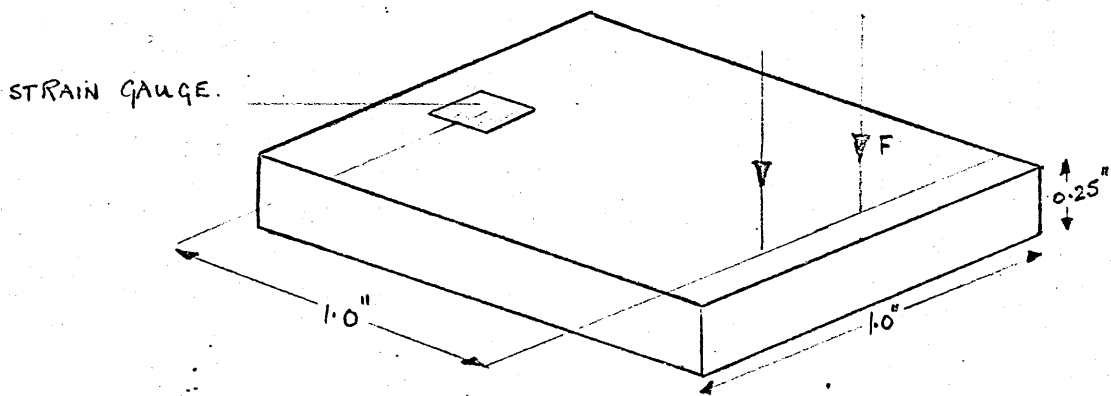


FIG. A 3:2 CANTILEVER DIMENSIONS

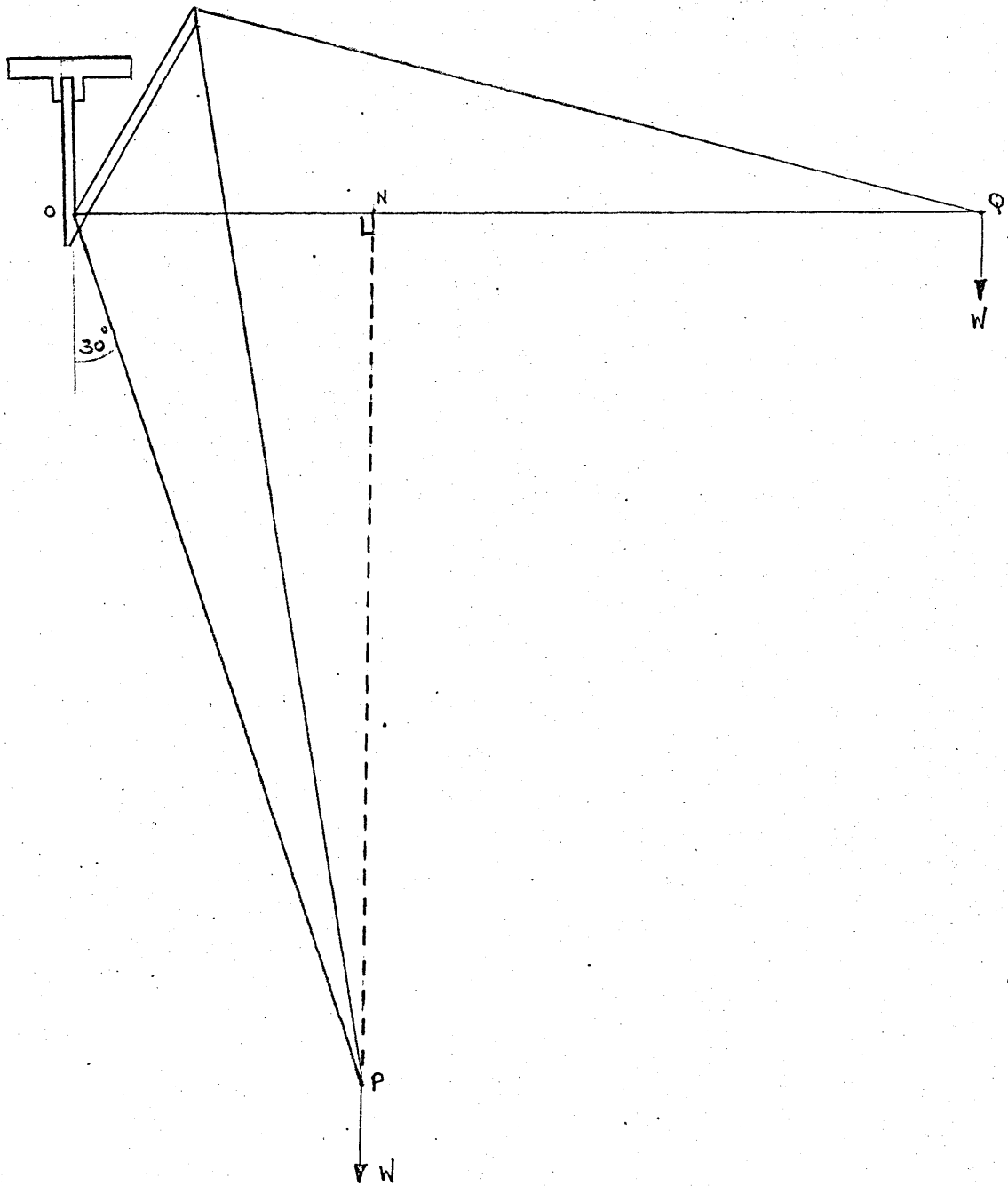
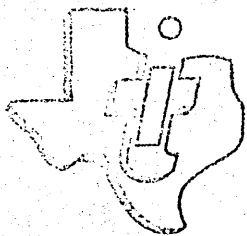


FIG. A3-3 MAXIMUM AND MINIMUM BENDING MOMENT

INTEGRATED CIRCUITS

NEW PRODUCT BULLETIN



This announcement provides preliminary engineering information on new Texas Instruments products. Definitive specifications are now being prepared for publication.

TI  
SEMICONDUCTOR NETWORKS<sup>†</sup>

TYPE SN7490N  
DECADE COUNTER

A SERIES 74N TTL HIGH-SPEED DECADE COUNTER  
FOR APPLICATION IN

- Digital Computer Systems
- Data Handling Systems
- Control Systems

logic

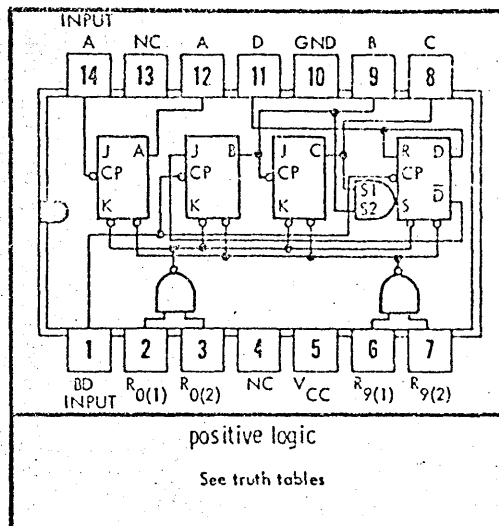
TRUTH TABLES

BCD COUNT SEQUENCE  
(See Note 1)

COUNT	OUTPUT			
	D	C	B	A
0	0	0	0	0
1	0	0	0	1
2	0	0	1	0
3	0	0	1	1
4	0	1	0	0
5	0	1	0	1
6	0	1	1	0
7	0	1	1	1
8	1	0	0	0
9	1	0	0	1

RESET/COUNT (See Note 2)

RESET INPUTS				OUTPUT
R <sub>0</sub> (1)	R <sub>0</sub> (2)	R <sub>9</sub> (1)	R <sub>9</sub> (2)	
1	1	0	X	0 0 0 0
1	1	X	0	0 0 0 0
X	X	1	1	1 0 0 1
X	0	X	0	COUNT
0	X	0	X	COUNT
0	X	X	0	COUNT
X	0	0	X	COUNT



- NOTES: 1. Output A connected to input BD for BCD count.  
2. X indicates that either a logical 1 or a logical 0 may be present.

description and typical count configurations

The SN7490N is a high-speed, monolithic decade counter consisting of four dual-rank, master-slave flip-flops internally interconnected to provide a divide-by-two counter and a divide-by-five counter. Gated direct reset lines are provided to inhibit count inputs and return all outputs to a logical zero or to a binary coded decimal (BCD) count of 9. As the output from flip-flop A is not internally connected to the succeeding stages, the count may be separated in three independent count modes:

1. When used as a binary coded decimal decade counter, the BD Input must be externally connected to the A output. The A Input receives the incoming count, and a count sequence is obtained in accordance with the BCD count sequence truth table shown above. In addition to a conventional zero reset, inputs are provided to reset a BCD 9 count for nine's complement decimal applications.
2. If a symmetrical divide-by-ten count is desired for frequency synthesizers or other applications requiring division of a binary count by a power of ten, the D output must be externally connected to the A Input. The Input count is then applied at the BD Input and a divide-by-ten square wave is obtained at output A.
3. For operation as a divide-by-two counter and a divide-by-five counter, no external interconnections are required. Flip-flop A is used as a binary element for the divide-by-two function. The BD Input is used to obtain binary divide-by-five operation at the B, C, and D outputs. In this mode, the two counters operate independently; however, all four flip-flops are reset simultaneously.

The SN7490N is completely compatible with Series 74 and Series 74 930-TTL, and Series 15 830 DTL logic families. Average power dissipation is 160 mW.

† Patented by Texas Instruments

IDENTICAL TO: SC 9435A  
FEBRUARY 1967

# TYPE 5117400N DECADÉ COUNTER

absolute maximum ratings over operating free-air temperature range (unless otherwise noted)

Supply Voltage $V_{CC}$ (See Note 3)	7 V
Input Voltage $V_{in}$ (See Notes 3 and 4)	5.5 V
Operating Free-Air Temperature Range	0°C to 70°C
Storage Temperature Range	-55°C to 125°C

- NOTES: 3. These voltage values are with respect to network ground terminal.  
4. Input signals must be zero or positive with respect to network ground terminal.

recommended operating conditions

Supply Voltage $V_{CC}$	4.75 V to 5.25 V
Fan-Out From Each Output (See Note 5)	1 to 10
Width of Input Count Pulse, $t_{p(in)}$	$\geq 50$ ns
Width of Reset Pulse, $t_{p(reset)}$	$\geq 50$ ns

NOTE 5: Fan-out from output A to input BD and to 10 additional Series 74 loads is permitted.

electrical characteristics,  $T_A = 0^\circ\text{C}$  to  $70^\circ\text{C}$

PARAMETER	TEST FIG.	TEST CONDITIONS	MIN	TYP	MAX	UNIT
$V_{in(1)}$ Input voltage required to ensure logical 1 at inputs A, $R_{0(1)}$ , $R_{0(2)}$ , $R_{9(1)}$ , and $R_{9(2)}$	1	$V_{CC} = 4.75$ V	2			V
$V_{in(1)}$ Input voltage required to ensure logical 1 at input BD	1	$V_{CC} = 4.75$ V	2.2			V
$V_{in(0)}$ Input voltage required to ensure logical 0 at inputs A, $R_{0(1)}$ , $R_{0(2)}$ , $R_{9(1)}$ , and $R_{9(2)}$	2	$V_{CC} = 4.75$ V			0.8	V
$V_{in(0)}$ Input voltage required to ensure logical 0 at input BD	2	$V_{CC} = 4.75$ V			0.6	V
$V_{out(1)}$ Logical 1 output voltage	2	$V_{CC} = 4.75$ V, $I_{load} = -400$ $\mu$ A	2.4			V
$V_{out(0)}$ Logical 0 output voltage	1	$V_{CC} = 4.75$ V, $I_{sink} = 16$ mA			0.4	V
$I_{in(1)}$ Logical 1 level input current at $R_{0(1)}$ , $R_{0(2)}$ , $R_{9(1)}$ , or $R_{9(2)}$	3	$V_{CC} = 5.25$ V, $V_{in} = 2.4$ V			40	$\mu$ A
		$V_{CC} = 5.25$ V, $V_{in} = 5.5$ V			1	mA
$I_{in(1)}$ Logical 1 level input current at input A	3	$V_{CC} = 5.25$ V, $V_{in} = 2.4$ V			80	$\mu$ A
		$V_{CC} = 5.25$ V, $V_{in} = 5.5$ V			1	mA
$I_{in(1)}$ Logical 1 level input current at input BD	3	$V_{CC} = 5.25$ V, $V_{in} = 2.4$ V			160	$\mu$ A
		$V_{CC} = 5.25$ V, $V_{in} = 5.5$ V			1	mA
$I_{in(0)}$ Logical 0 level input current at $R_{0(1)}$ , $R_{0(2)}$ , $R_{9(1)}$ , or $R_{9(2)}$	4	$V_{CC} = 5.25$ V, $V_{in} = 0.4$ V			-1.6	mA
$I_{in(0)}$ Logical 0 level input current at input A	4	$V_{CC} = 5.25$ V, $V_{in} = 0.4$ V			-3.2	mA
$I_{in(0)}$ Logical 0 level input current at input BD	4	$V_{CC} = 5.25$ V, $V_{in} = 0.4$ V			-6.4	mA
$I_{OS}$ Short-circuit output current†	5	$V_{CC} = 5.25$ V, $V_{out} = 0$ V	-18		-57	mA
$I_{CC}$ Supply Current	3	$V_{CC} = 5$ V, $T_A = 25^\circ\text{C}$		32		mA

† Not more than one output should be shorted at a time.

switching characteristics,  $V_{CC} = 5$  V,  $T_A = 25^\circ\text{C}$ ,  $N = 10$

PARAMETER	TEST FIG.	TEST CONDITIONS	MIN	TYP	MAX	UNIT
$f_{max}$ Maximum frequency of input count pulses			10	18		MHz
$t_{pd1}$ Propagation delay time to logical 1 level from input count pulse to output C	6			60	100	ns
$t_{pd0}$ Propagation delay time to logical 0 level from input count pulse to output C	6			60	100	ns

**μA710**

**HIGH SPEED DIFFERENTIAL COMPARATOR**

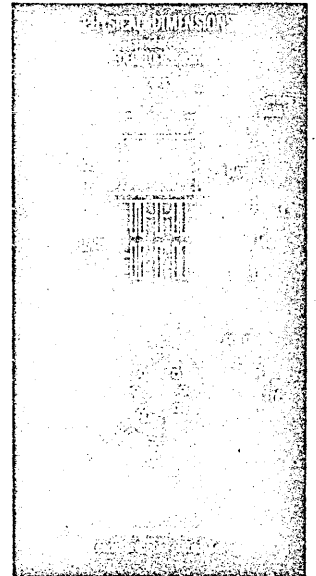
SILICON PLANAR LINEAR INTEGRATED CIRCUIT

EXTENDED TEMPERATURE RANGE -55°C to +125°C

**GENERAL DESCRIPTION** - The μA710 is a differential voltage comparator intended for applications requiring high accuracy and fast response times. It is constructed on a single silicon chip using the Fairchild Planar epitaxial process. The device is useful as a variable threshold Schmitt trigger, a pulse height discriminator, a voltage comparator in high-speed A-D converters, a memory sense amplifier or a high-noise immunity line receiver. The output of the comparator is compatible with all integrated logic forms.

**ABSOLUTE MAXIMUM RATINGS**

Positive Supply Voltage	+ 14 V
Negative Supply Voltage	- 7 V
Peak Output Current	10 mA
Differential Input Voltage	± 5 V
Input Voltage	± 7 V
Internal Power Dissipation	
TO-5 (Note 1)	300 mW
Flat Package (Note 2)	200 mW
Operating Temperature Range	-55°C to + 125°C
Storage Temperature Range	-65°C to + 150°C
Lead Temperature (Soldering, 60 sec)	+ 300°C

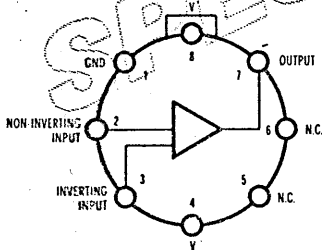


PART NO. U5B771031X

Notes on page 2

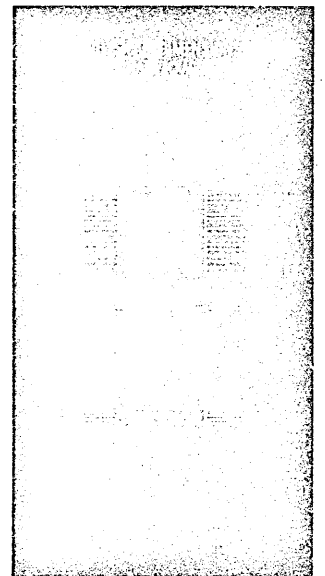
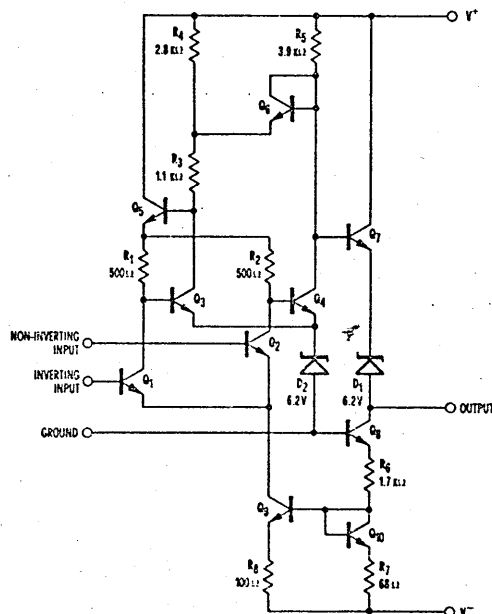
**TO-5 CONNECTION DIAGRAM**

(top view)



Note: Pin 4 connected to case.

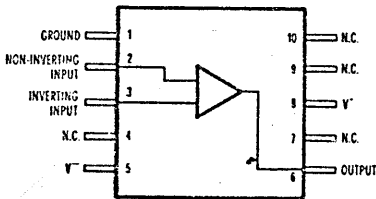
**SCHEMATIC DIAGRAM**



PART NO. U3H771031X

**FLAT PACKAGE CONNECTION DIAGRAM**

(top view)



SGS-FAIRCHILD, LONDON · MILAN · PARIS · STOCKHOLM · STUTTGART



# μA710 SGS-Fairchild Silicon Planar Linear Integrated Circuit

## ELECTRICAL CHARACTERISTICS ( $T_A = +25^\circ\text{C}$ , $V^+ = 12\text{V}$ , $V^- = -6\text{V}$ unless otherwise specified)

PARAMETER (see definitions)	CONDITIONS (Note 4)	MIN.	TYP.	MAX.	UNIT
Input Offset Voltage	$R_S \leq 200\ \Omega$		0.6	2	mV
Input Offset Current			0.75	3	μA
Input Bias Current			13	20	μA
Voltage Gain		1250	1700		
Output Resistance			200		Ω
Output Sink Current	$\Delta V_{in} \geq 5\text{mV}$ , $V_{out} = 0$	2	2.5		mA
Response Time (Note 3)			40		ns
The following specifications apply for $-55^\circ\text{C} \leq T_A \leq +125^\circ\text{C}$ :					
Input Offset Voltage	$R_S \leq 200\ \Omega$			3	mV
Average Temperature Coefficient of Input Offset Voltage	$R_S = 50\ \Omega$ $T_A = 25^\circ\text{C}$ to $T_A = 125^\circ\text{C}$ $T_A = 25^\circ\text{C}$ to $T_A = -55^\circ\text{C}$		3.5 2.7	10 10	μV/°C μV/°C
Input Offset Current	$T_A = +125^\circ\text{C}$ $T_A = -55^\circ\text{C}$		0.25 1.8	3 7	μA μA
Average Temperature Coefficient of Input Offset Current	$T_A = 25^\circ\text{C}$ to $T_A = +125^\circ\text{C}$ $T_A = 25^\circ\text{C}$ to $T_A = -55^\circ\text{C}$		5 15	25 75	nA/°C nA/°C
Input Bias Current	$T_A = -55^\circ\text{C}$		27	45	μA
Input Voltage Range	$V^- = -7\text{V}$	$\pm 5$			V
Common Mode Rejection Ratio	$R_S \leq 200\ \Omega$	80	100		dB
Differential Input Voltage Range		$\pm 5$			V
Voltage Gain		1000			
Positive Output Level	$\Delta V_{in} \geq 5\text{mV}$ , $0 \leq I_{out} \leq 5\text{mA}$	2.5	3.2	4	V
Negative Output Level	$\Delta V_{in} \geq 5\text{mV}$	-1	-0.5	0	V
Output Sink Current	$\Delta V_{in} \geq 5\text{mV}$ , $V_{out} = 0$ $T_A = +125^\circ\text{C}$ $T_A = -55^\circ\text{C}$	0.5 1	1.7 2.3		mA mA
Positive Supply Current	$V_{out} \leq 0$		5.2	9	mA
Negative Supply Current			4.6	7	mA
Power Consumption			90	150	mW

### NOTES:

- (1) Rating applies for case temperatures to  $+125^\circ\text{C}$ ; derate linearly at  $6.6\text{ mW}/^\circ\text{C}$  for ambient temperatures above  $+105^\circ\text{C}$ .
- (2) Derate linearly at  $4\text{ mW}/^\circ\text{C}$  for ambient temperatures above  $+100^\circ\text{C}$ .
- (3) The response time specified (see definitions) is for a  $100\text{ mV}$  input step with  $5\text{mV}$  overdrive.
- (4) The input offset voltage and input offset current (see definitions) are specified for a logic threshold voltage of  $1.8\text{V}$  at  $-55^\circ\text{C}$ ,  $1.4\text{V}$  at  $+25^\circ\text{C}$  and  $1\text{V}$  at  $+125^\circ\text{C}$ .

HIGH GAIN, WIDEBAND DC AMPLIFIER - SILICON PLANAR LINEAR INTEGRATED CIRCUIT

**μA702C**

**HIGH GAIN, WIDEBAND DC AMPLIFIER**

SILICON PLANAR LINEAR INTEGRATED CIRCUIT

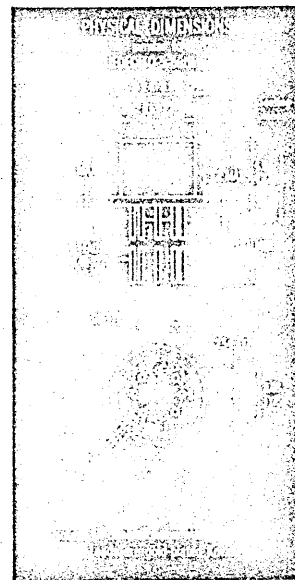
STANDARD TEMPERATURE RANGE 0°C to 70°C

**GENERAL DESCRIPTION** - The μA702C is a complete DC amplifier constructed on a single silicon chip, using the Fairchild Planar epitaxial process. It is intended for use as an operational amplifier in high speed analog computers, as a precision instrumentation amplifier, or in other applications requiring a feedback amplifier useful from DC to 30 MHz. For extended temperature range operation (-55°C to 125°C) see μA702 data sheet.

**ABSOLUTE MAXIMUM RATINGS**

Total Supply Voltage Between V <sup>+</sup> and V <sup>-</sup> Terminals	21 V
Peak Load Current	50 mA
Internal Power Dissipation (Note 1)	300 mW
(TO-5)	200 mW
(Flat Package)	-65°C to 150°C
Storage Temperature Range	0°C to 70°C
Operating Temperature Range	± 5 V
Differential Input Voltage	1.5 V to -6 V
Input Voltage, Either Input	300°C
Lead Temperature (Soldering, 60 sec)	

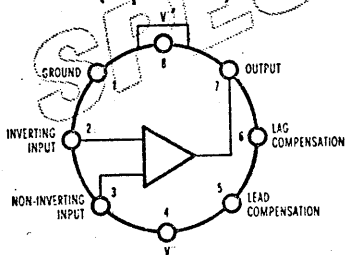
NOTE 1: Rating applies for ambient temperature to 70°C.



PART NO. U5B771239X

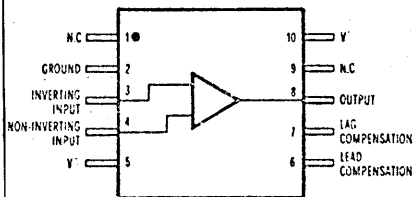
**TO-5 CONNECTION DIAGRAM**

(top view)

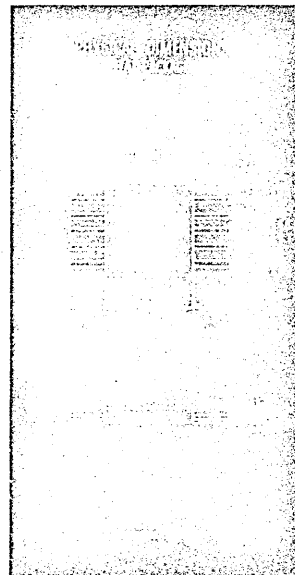
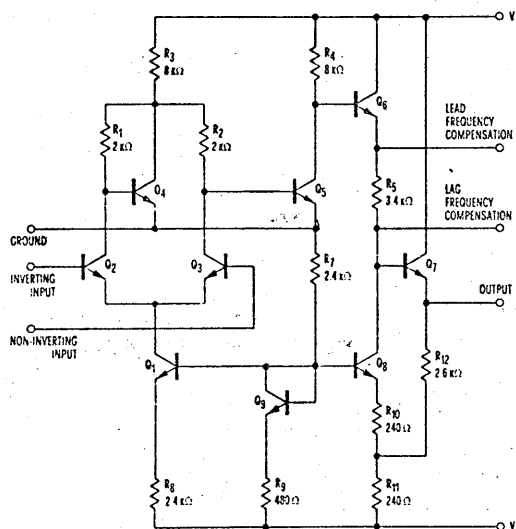


Note: Pin 4 connected to case

**FLAT PACKAGE CONNECTION DIAGRAM**  
(top view)



**SCHEMATIC DIAGRAM**



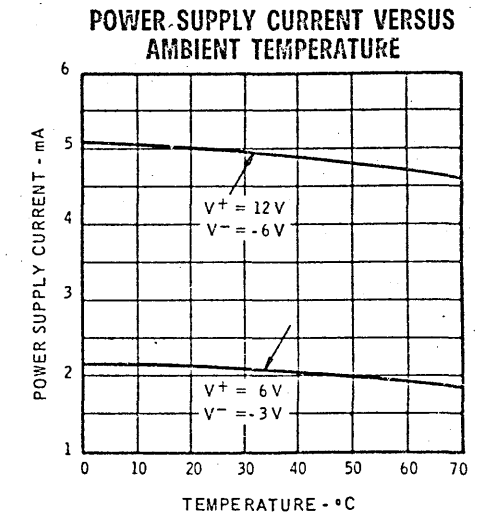
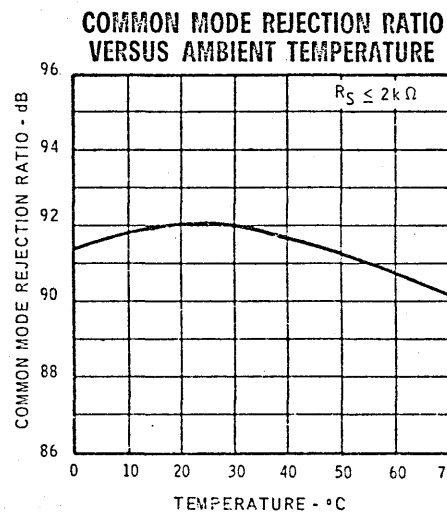
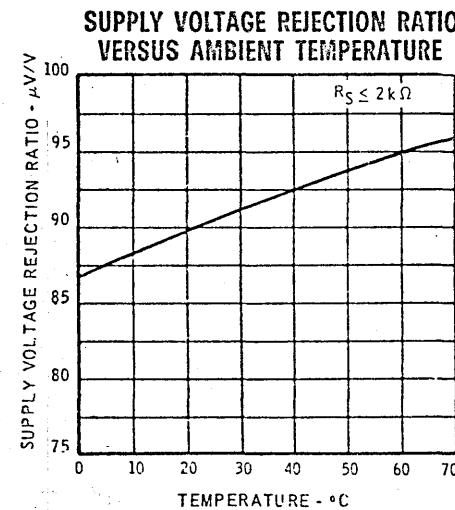
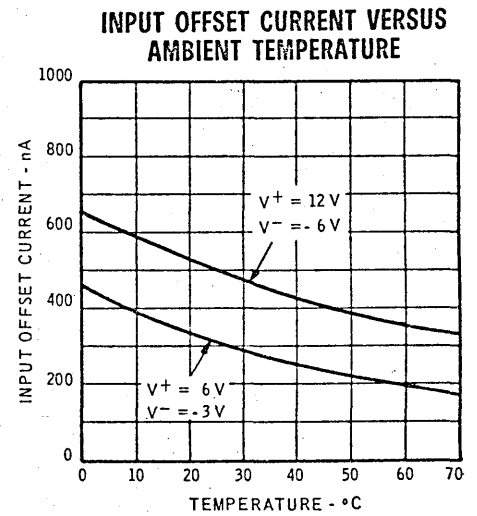
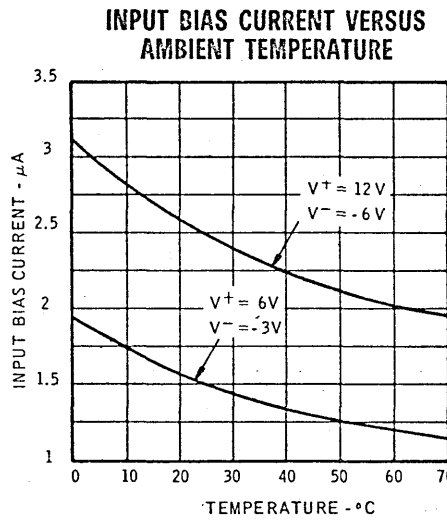
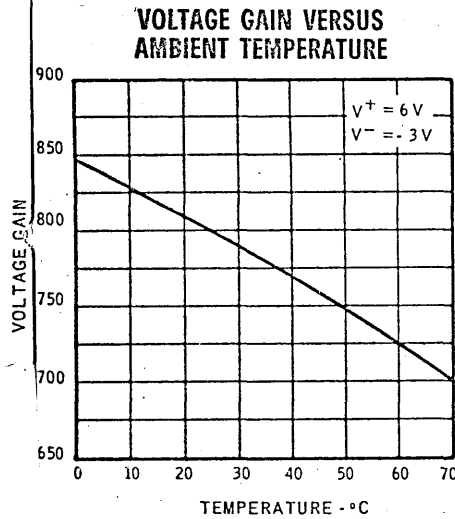
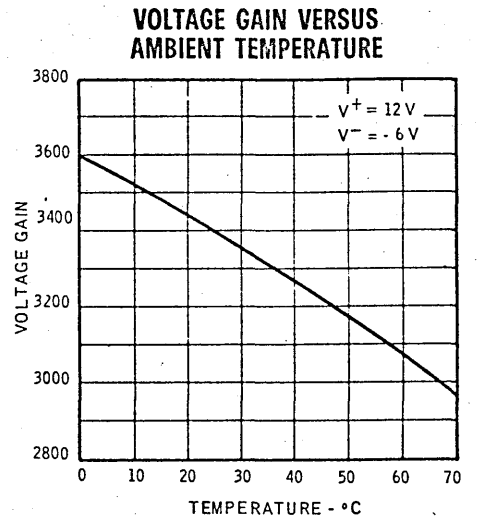
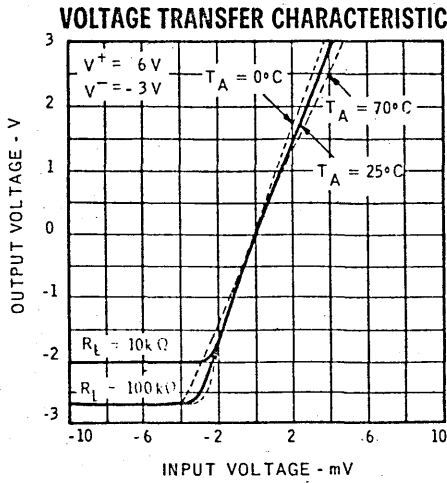
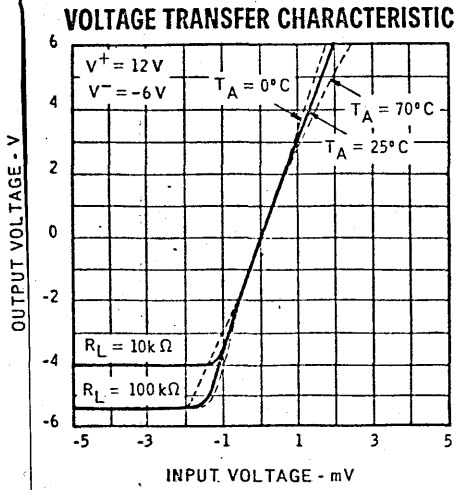
PART NO. U3H771239X

# μA702C SGS-Fairchild Silicon Planar Linear Integrated Circuit

## ELECTRICAL CHARACTERISTICS ( $T_A = 25^\circ\text{C}$ unless otherwise specified)

PARAMETER (see definitions)	CONDITIONS	$V^+ = 12\text{V}, V^- = -6\text{V}$			$V^+ = 6\text{V}, V^- = -3\text{V}$			UNIT
		MIN.	TYP.	MAX.	MIN.	TYP.	MAX.	
Input Offset Voltage	$R_S \leq 2\text{k}\Omega$		1.5	5		1.7	6	mV
Input Offset Current			0.5	2		0.3	2	$\mu\text{A}$
Input Bias Current			2.5	7.5		1.5	5	$\mu\text{A}$
Input Resistance		10	32		16	55		$\text{k}\Omega$
Input Voltage Range		-4		0.5	-1.5		0.5	V
Common Mode Rejection Ratio	$R_S \leq 2\text{k}\Omega, f \leq 1\text{kHz}$	70	92		70	92		dB
Large-Signal Voltage Gain	$R_L \geq 100\text{k}\Omega, V_{\text{out}} = \pm 5\text{V}$	2000	3400	6000				
	$R_L \geq 100\text{k}\Omega, V_{\text{out}} = \pm 2.5\text{V}$				500	800	1500	
Output Resistance			200	600		300	800	$\Omega$
Supply Current	$V_{\text{out}} = 0$		5	6.7		2.1	3.3	mA
Power Consumption	$V_{\text{out}} = 0$		90	120		19	30	mW
Transient Response (unity gain)	$C_1 = 0.01\ \mu\text{F}, R_1 = 20\ \Omega$ $R_L \leq 100\text{k}\Omega, V_{\text{in}} = 10\text{mV}$							
Risetime			25	120				ns
Overshoot	$C_L \leq 100\text{pF}$		10	50				%
Transient Response (x 100 gain)	$C_3 = 50\text{pF}, R_L \geq 100\text{k}\Omega,$ $V_{\text{in}} = 1\text{mV}$							
Risetime			10	30				ns
Overshoot			20	40				%
The following specifications apply for $0^\circ\text{C} \leq T_A \leq 70^\circ\text{C}$ :								
Input Offset Voltage	$R_S \leq 2\text{k}\Omega$			6.5			7.5	mV
Average Temperature Coefficient of Input Offset Voltage	$R_S = 50\ \Omega$ $T_A = 70^\circ\text{C}$ to $T_A = 0^\circ\text{C}$		5	20		7.5	25	$\mu\text{V}/^\circ\text{C}$
Input Offset Current				2.5			2.5	$\mu\text{A}$
Average Temperature Coefficient of Input Offset Current	$T_A = 25^\circ\text{C}$ to $T_A = 70^\circ\text{C}$ $T_A = 25^\circ\text{C}$ to $T_A = 0^\circ\text{C}$		4	10		3	8	$\text{nA}/^\circ\text{C}$
Input Bias Current	$T_A = 0^\circ\text{C}$		6	20		5.5	18	$\text{nA}/^\circ\text{C}$
Input Resistance		6	18		9	27		$\text{k}\Omega$
Common Mode Rejection Ratio	$R_S \leq 2\text{k}\Omega, f \leq 1\text{kHz}$	65	86		65	86		dB
Supply Voltage Rejection Ratio	$V^+ = 12\text{V}, V^- = 6\text{V}$ to $V^+ = 6\text{V}, V^- = 3\text{V}$ $R_S \leq 2\text{k}\Omega$		90	300		90	300	$\mu\text{V}/\text{V}$
Large-Signal Voltage Gain	$R_L \geq 100\text{k}\Omega, V_{\text{out}} = \pm 5\text{V}$	1500		7000				
	$R_L \geq 100\text{k}\Omega, V_{\text{out}} = \pm 2.5\text{V}$				400		1750	
Output Voltage Swing	$R_L \geq 100\text{k}\Omega$	$\pm 5$	$\pm 5.3$		$\pm 2.5$	$\pm 2.7$		V
	$R_L \geq 10\text{k}\Omega$	$\pm 3.5$	$\pm 4$		$\pm 1.5$	$\pm 2$		V
Supply Current	$V_{\text{out}} = 0$		5	7		2.1	3.9	mA
Power Consumption	$V_{\text{out}} = 0$		90	125		19	35	mW

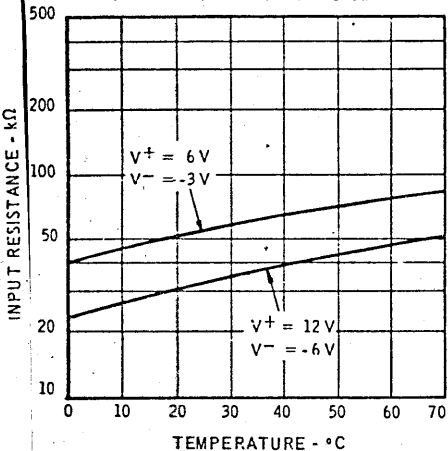
TYPICAL ELECTRICAL CHARACTERISTICS (25°C free air temperature unless otherwise noted)



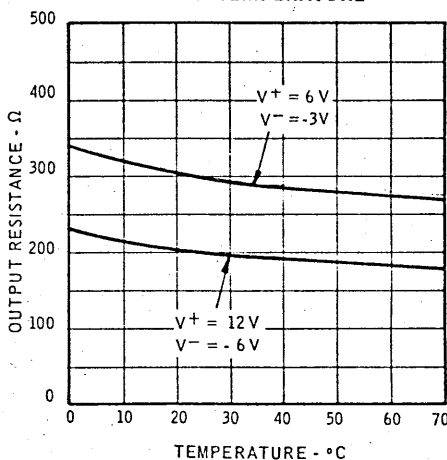
# μA702C SGS-Fairchild Silicon Planar Linear Integrated Circuit

TYPICAL ELECTRICAL CHARACTERISTICS (25°C free air temperature unless otherwise noted)

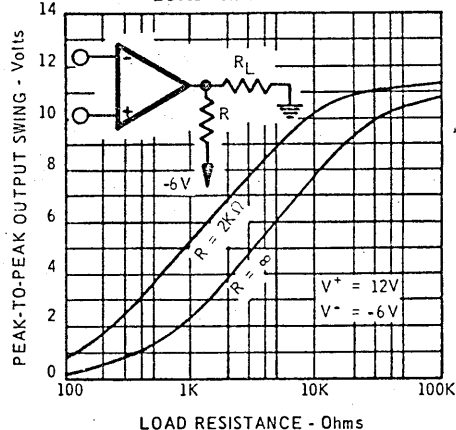
**INPUT RESISTANCE VERSUS AMBIENT TEMPERATURE**



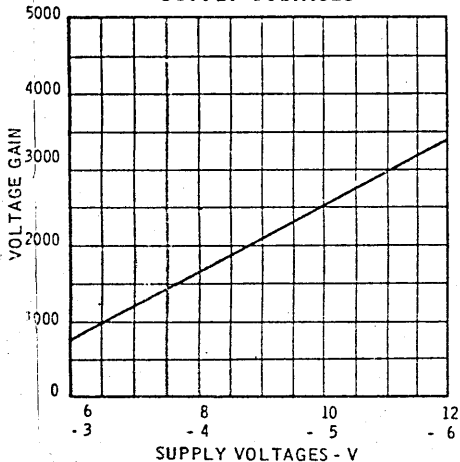
**OUTPUT RESISTANCE VERSUS AMBIENT TEMPERATURE**



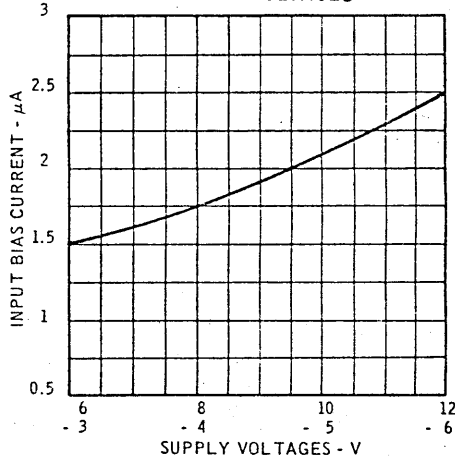
**OUTPUT VOLTAGE SWING VERSUS LOAD RESISTANCE**



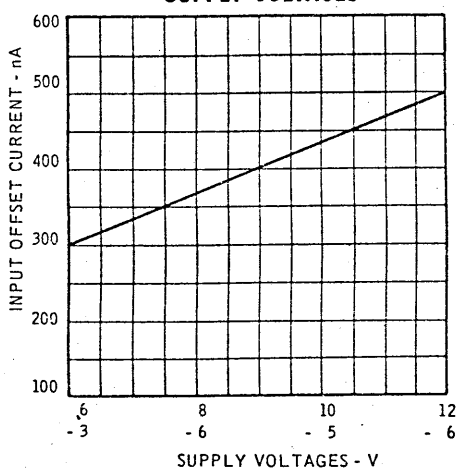
**VOLTAGE GAIN VERSUS SUPPLY VOLTAGES**



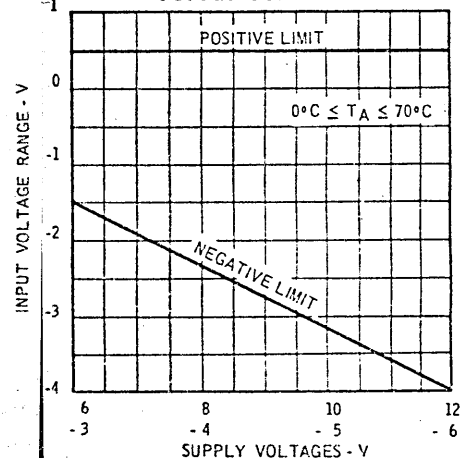
**INPUT BIAS CURRENT VERSUS SUPPLY VOLTAGES**



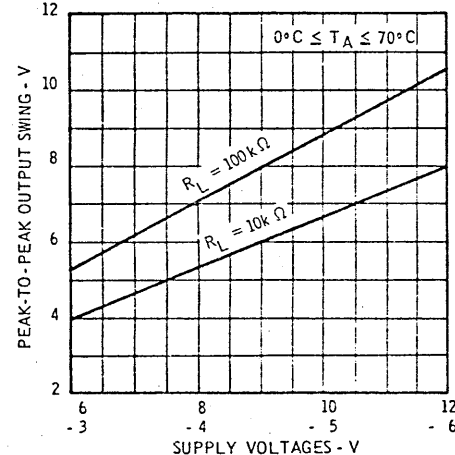
**INPUT OFFSET CURRENT VERSUS SUPPLY VOLTAGES**



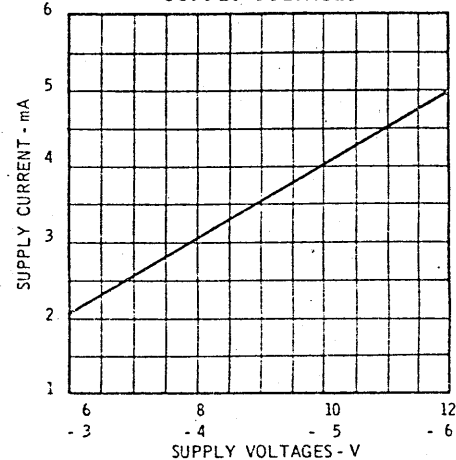
**INPUT VOLTAGE RANGE VERSUS SUPPLY VOLTAGES**



**OUTPUT VOLTAGE SWING VERSUS SUPPLY VOLTAGES**

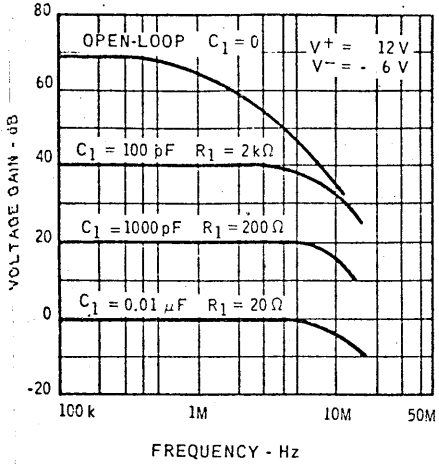


**SUPPLY CURRENT VERSUS SUPPLY VOLTAGES**

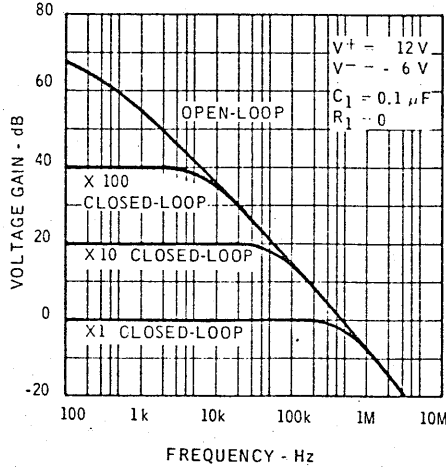


## TYPICAL ELECTRICAL CHARACTERISTICS (25°C free air temperature unless otherwise noted)

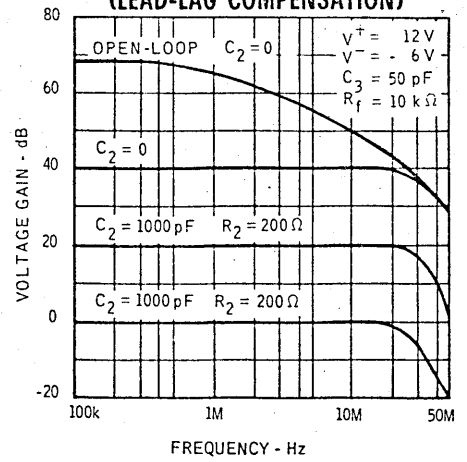
### FREQUENCY RESPONSE FOR VARIOUS CLOSED-LOOP GAINS (LAG COMPENSATION)



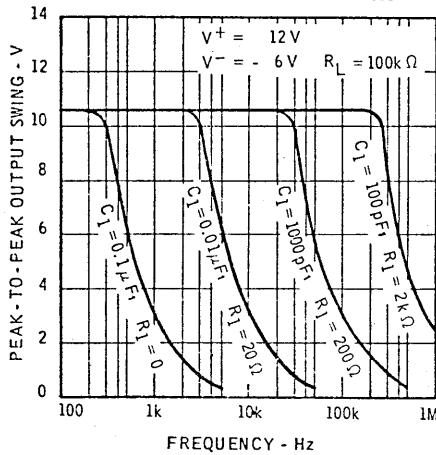
### FREQUENCY RESPONSE WITH CONSERVATIVE COMPENSATION NETWORK



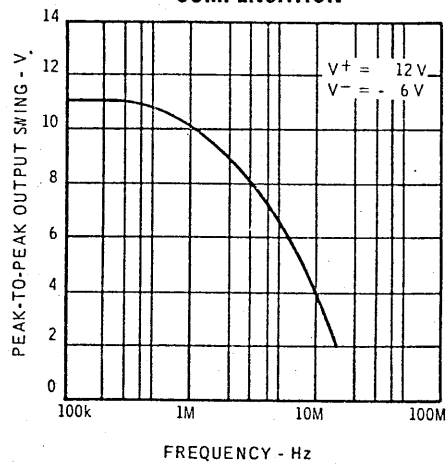
### FREQUENCY RESPONSE FOR VARIOUS CLOSED-LOOP GAINS (LEAD-LAG COMPENSATION)



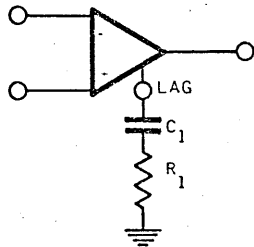
### OUTPUT VOLTAGE SWING VERSUS FREQUENCY FOR VARIOUS LAG COMPENSATION NETWORKS



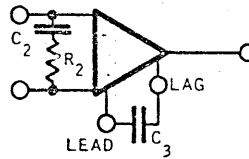
### OUTPUT VOLTAGE SWING VERSUS FREQUENCY WITH LEAD-LAG COMPENSATION



### FREQUENCY COMPENSATION CIRCUITS



LAG COMPENSATION



LEAD-LAG COMPENSATION